Nature-inspired materials and structures using 3D Printing

Amit Bandyopadhyay and Kellen D. Traxel
W. M. Keck Biomedical Materials Research Laboratory
School of Mechanical and Materials Engineering
Washington State University, Pullman, WA 99164, USA.
E-mail: amitband@wsu.edu

Abstract

Emulating the unique combination of structural, compositional, and functional gradation in natural materials is exceptionally challenging. Many natural structures have proved too complex or expensive to imitate using traditional processing techniques despite recent advances. Recent innovations within the field of additive manufacturing (AM) or 3D Printing (3DP) have shown the ability to create structures that have variations in material composition, structure, and performance, providing a new design-for-manufacturing platform for the imitation of natural materials. AM or 3DP techniques are capable of manufacturing structures that have significantly improved properties and functionality over what could be traditionally-produced, giving manufacturers an edge in their ability to realize components for highly-specialized applications in different industries. To this end, the present work reviews fundamental advances in the use of naturally-inspired design enabled through 3DP / AM, how these techniques can be further exploited to reach new application areas and the challenges that lie ahead for widespread implementation. An example of how these techniques can be applied towards a total hip arthroplasty application is provided to spur further innovation in this area.

Keywords: Natural structures; 3D Printing; additive manufacturing; hybrid materials; hybrid manufacturing.

1. Introduction

Nature has undoubtedly proven itself the most incredible designer, fabricator, and refiner of structural materials across all length scales. While traditional human-centered materials design requires optimization of factors such as strength and ductility, or fracture toughness and stiffness, among many other examples, recent work has shown that structures found in Nature often break down those barriers, producing materials with significantly improved properties over anything designed by humans [1]. In some cases, these natural structures combine a hierarchical microstructure of hard and soft phases that increase both the strength and toughness of materials, without increasing one at the expense of the other, or create unique geometrical features to significantly improve over previous designs only through evolution (see **Fig. 1**). This capability is quite elusive in many industrial structural applications and has spurred significant development into understanding the underlying mechanisms behind such behavior via testing and analysis (see **Fig. 2A**) [2]. Until now, achieving intricate designs such as in bone and nacre, among others, has been nearly impossible with traditional manufacturing approaches due to complex reinforcing mechanisms not producible with current technologies. Even with an advanced laboratory setup, the challenge of emulating these materials stems from their natural-fabrication process beginning at the nanometer level via complex templating mechanisms. However, the most practical manufacturing is accomplished on the macro and sometimes micro-scale(s) structural components [3]. In bone, nacre, and enamel, as prime structural examples, nanometer-sized reinforcement grains increase strength and an overall decrease in stress-concentrations resulting in properties not achievable with traditionally-conceived composites [4].

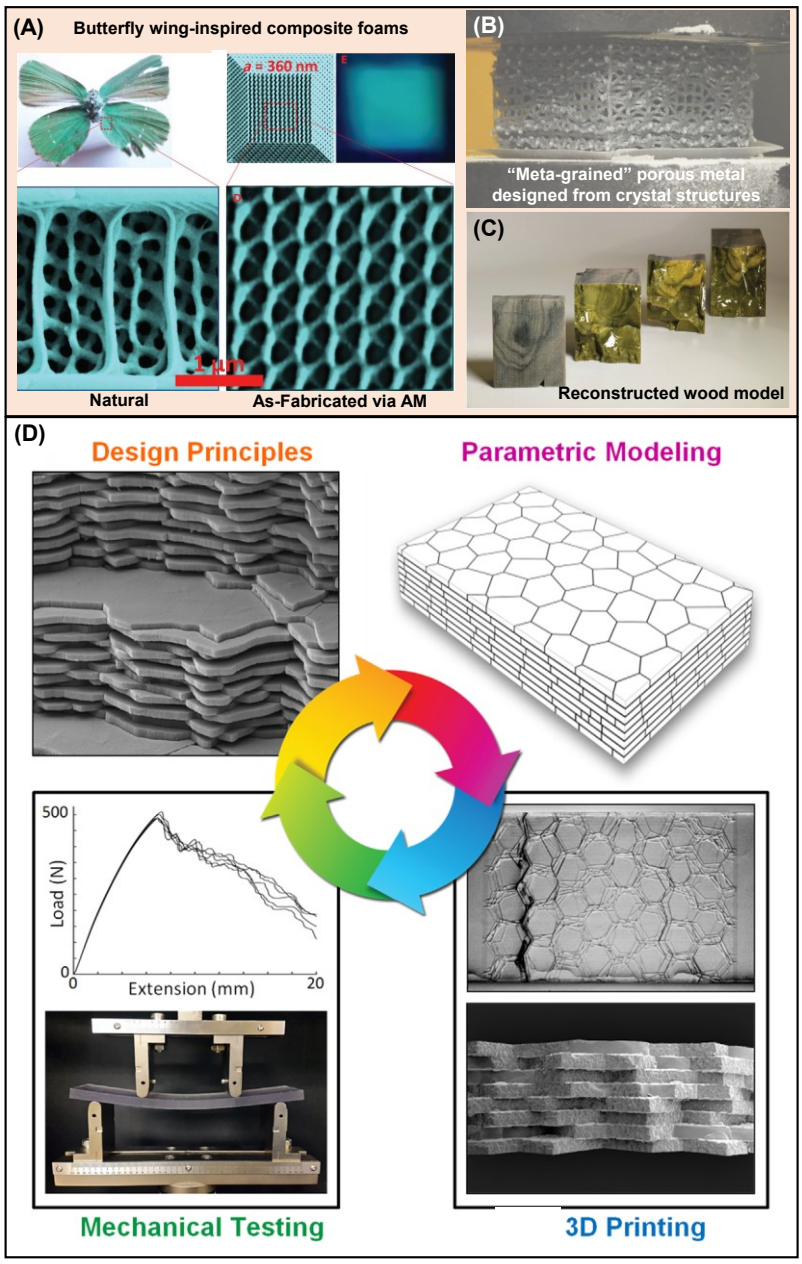

Figure 1: Examples of additive manufacturing innovation by mimicking natural materials and designs. **(A)** Synthetic butterfly wings with nano-scale features manufactured using two-beam lithography [10]. **(B)** Damage-resistant meta-grained metal comprised of lattices (~30 mm square cross section) designed based on fundamental crystal structures processed using powder-bed-fusion [11]. **(C)** Wood models (~several cm in size) printed in full color from successive sectional scans using Polyjet processing technology [12]. **(D)** Concept diagram showing the design-processing-properties process when analyzing naturally-inspired structures [17].

Even on the larger-scale, however, traditional fabrication of comparable architectures to natural structures is challenging as there is typically a scaling issue (natural materials are typically templated on the nanometer scale) as well as a material compatibility issue (processing of multiple materials into a single component is highly challenging using traditional methods). While tape and/or freeze-casting [5], templating [6], lithography [7], "layer by layer" assembly [8], among other traditional processing routes [9], have been utilized to achieve a combination of structural and material variations within components, combining desirable microstructure, reinforcement morphology, and properties are

incredibly challenging at once due mainly to geometric restriction to samples such as plates/bars due to the precursor materials used in the traditional processes. While existing methods are capable of producing such structures with modifications as well as specific (and often expensive) equipment, recent additive-based manufacturing advancements have provided a platform for realizing multi-material architected components with a combination of complete geometric freedom and increased materials capability to create structures on a functional part scale and complexity. **Fig. 1A** shows work from Gan et al. (2016) involving a unique cellular butterfly-inspired structure processed via 3DP to understand the complex and often improved properties that this structural archetype has over others [10]. Other works from Pham et al. (2019) shown in **Fig. 1B**, and that of Stute et al. (2018) in **Fig. 1C** highlight other 3D Printing applications where natural materials are replicated to generate complex properties and characteristics [11,12]. These features are merely challenging, and sometimes impossible, to create using traditional methods. While future manufacturing and design innovation rely on the development of novel processing techniques for structures that are fully-optimized for their intended application, significant trade-offs are still imperative in the design process, motivating the exploration of such novel design-fabrication approaches that minimize trade-offs such as mimicking and understanding the performance of natural structures [13]. Schematics of current work in this area are shown in **Figs. 1D and 2A**, where natural structures are analyzed, emulated via computer-aided-design (CAD), and then processed and tested to understand the structures' properties and characteristics.

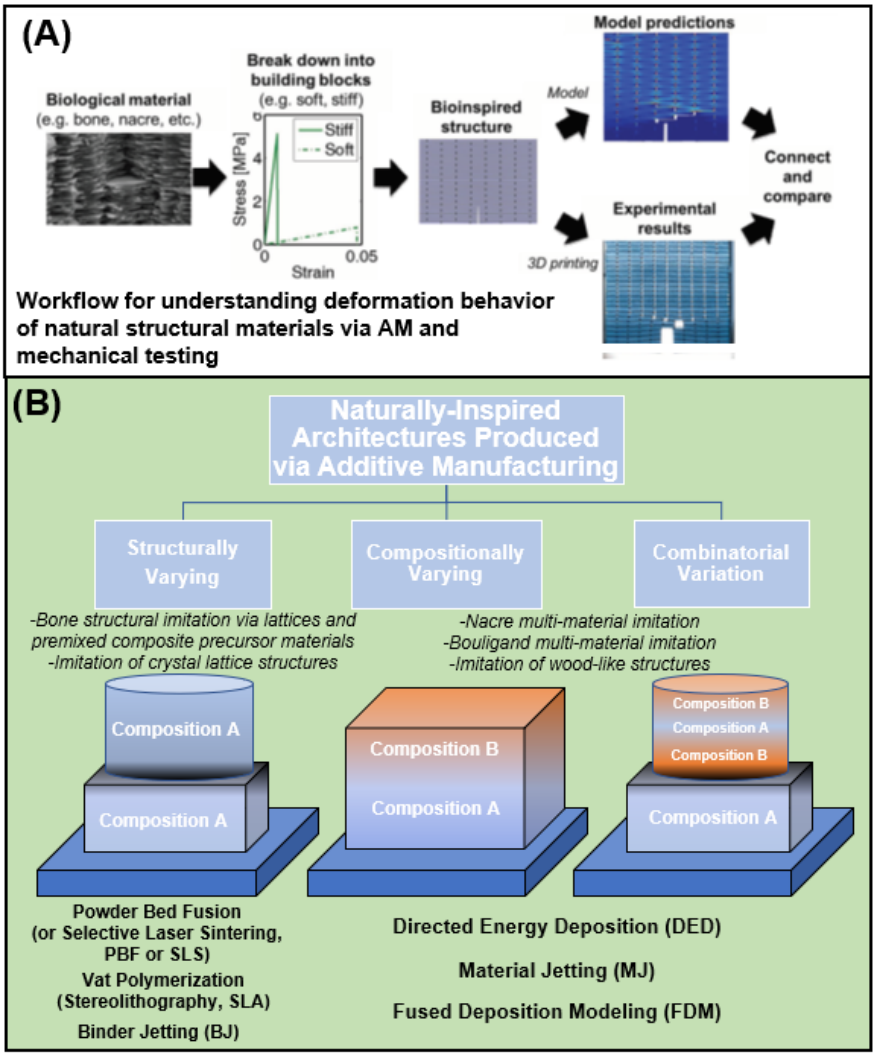

Figure 2: Classification of various naturally-inspired structures. **(A)** Schematic for understanding the deformation behavior of Nacre, samples processed using PolyJet and are on order of 50-65mm in size [31]. **(B)** Classification of naturally-inspired structures via composition and structural variations.

Additive manufacturing or 3D-Printing is a layer-by-layer process that enables engineers and researchers to conceive end-use parts from the ground-upwards. Instead of a wide array of parts being cast, injection-molded, machined, or forged, parts are shaped one layer at a time from the CAD model via a few highly-advanced methodologies. Despite the increasing adoption of additive-based processing into many different manufacturers' workflow, researchers and engineers are continuously finding areas to implement the technology to increase component functionality and/or geometric flexibility. In many cases, designers need to look no further than naturally-inspired architectures, where combinations of properties and materials have evolved organically and provide the highest performance possible within tight geometric windows. With the relative ease of changing structural and/or compositional

characteristics in structures via 3D Printing, the ability to exploit design strategies employed by natural structural materials has never been more achievable or exciting from an engineering design perspective, motivating investigations of the performance of these types of structures when processed via different 3D Printing avenues, as well as work that summarizes the current developments as a whole. **Fig. 2B** shows conceptually how much of the current work in 3D Printing of Nature-inspired structures have evolved. Depending on the material and process, natural structures have been mimicked from a compositional, structural, and combinatorial standpoint using 3D Printing technologies. Specifically, methods have been utilized to mimic structural variations in natural materials, whereas others mimic compositional variation, involving both composition and structural variation. Because of the different efforts, numerous 3D Printing methods have been utilized to achieve such structures, i.e., powder bed fusion, vat polymerization, and binder jetting (for structural variation), and directed energy deposition, material jetting, and fused deposition modeling (for compositional and combinatorial variation). Unique composite materials have often been fabricated, which emulate the natural structure, shedding light on researchers' design strategies in macroscale engineering applications. While recent review articles outline, some of the critical design and manufacturing aspects of these structures using traditional and/or additive-based approaches [14,15], the onset of multi-material AM techniques and variations of single-material techniques have elicited even more interest in emulating natural structures as well as biomimetic designs, which take concepts from Nature and apply them to simple engineering design and materials. Many research works describe the author's end results, but few discuss in detail the mechanics of printing these structures, what the main challenges are, or the future application areas could be, which is of the utmost importance to researchers developing next-generation materials and processing technologies. This work's main objectives are to overview what has been accomplished in the field of naturally-inspired

design via 3D Printing, the challenges in achieving these designs from a manufacturing perspective, and the next generation of components designed with natural strategies. To this end, the current work focuses on providing an overview of 3D Printing methods related to nature-inspired design and manufacturing, reviewing research works related to complex nature-inspired design through a summary of the author's findings and significance towards the field, and a look at the future trends and technologies relevant to the field. From our survey of the literature, several key structures have been widely-mimicked for structural design inspiration, namely, bone, nacre, and gyroidal structures, among others. Each of these architectures has its section within the review and an additional section reviewing other prominent works. An example case study shows how natural-structure mimicking can be incorporated into modern process workflows. This work is intended to demonstrate the efficacy of 3D Printing or additive manufacturing methods to create naturally-inspired structures not previously possible and inspire the next generation of design and manufacturing professionals.

2. Mimicking natural structures via 3D Printing

Varying both the composition and structure of materials within single components enables optimizing properties in site-specific locations like those observed in naturally-inspired structures such as nacre, bone, and Helicoid structures, among others (see **Fig. 2B**). These properties can be as fundamental as the density, strength, toughness, electrical/thermal conductivity, melting temperature, or as advanced as the biocompatibility, wear, corrosion, oxidation, or impact resistance. Although there are seven main categories of 3D Printing methods [16], several have been utilized in the literature to create structures with such

capabilities. These main methods for polymers, ceramics, and metals are summarized alongside a discussion of natural-structural emulation works using additive manufacturing (see **Table 1**).

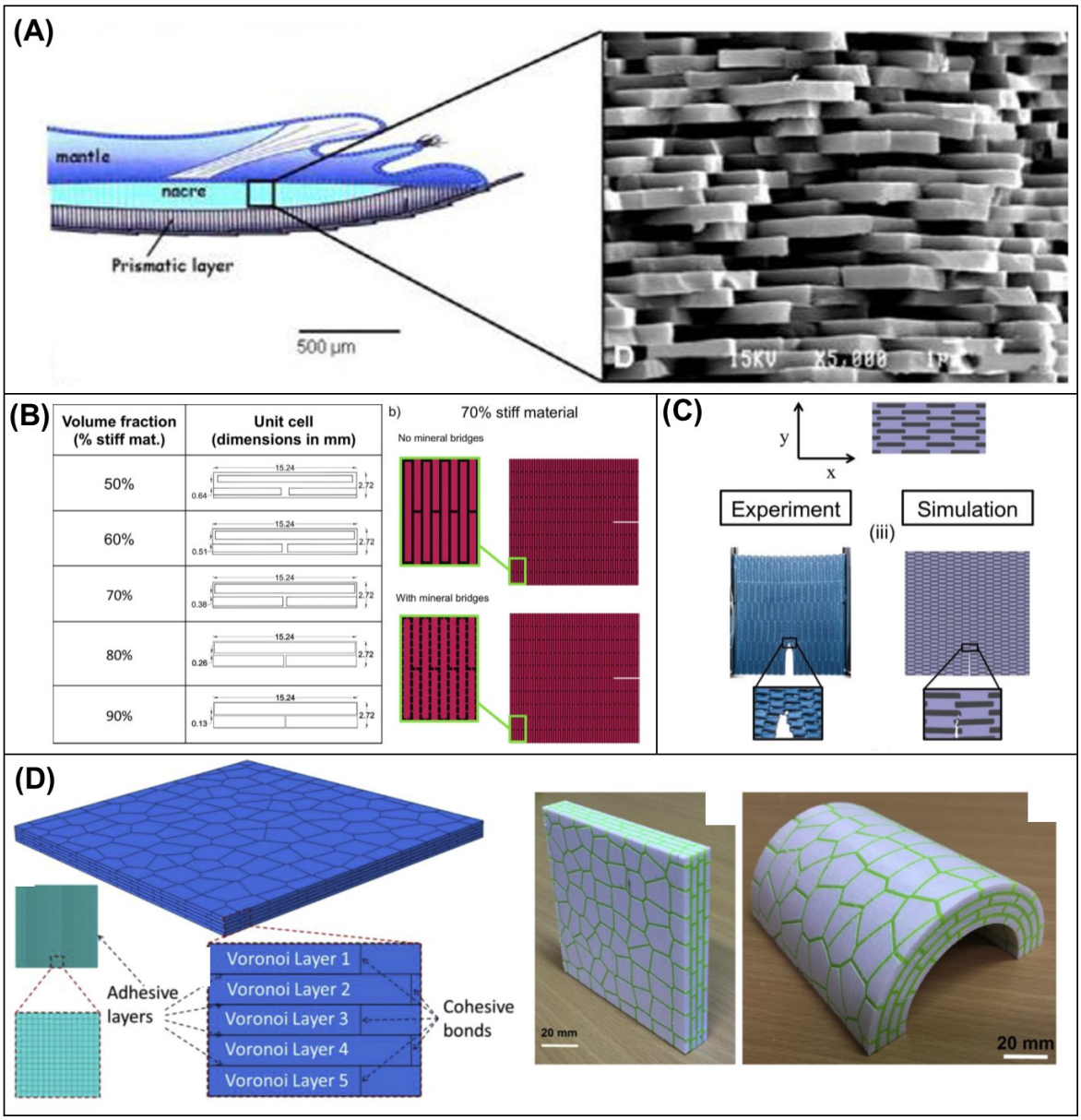

Figure 3: Additive manufacturing of nacre-like composite structures. **(A)** Structure of nacre at the nanometer scale showing the brick and mortar architecture, adapted from ref. [129]. **(B)** Design of nacre-composites using variable unit cell (repeating units) dimensions processed using PolyJet technique (note dimensions are in mm) [30]. **(C)** Comparison of experimental structural testing versus simulated performance in a nacre-inspired composite manufactured using PolyJet technology, adapted from ref. [31]. **(D)** Examples of brick and mortar nacre-like composite structures manufactured via FDM [32].

Table 1: Summary table of additive manufacturing methods and relevance to natural structure imitation and mimicking [13, 82].

ASTM Designation	Mechanism	Layer Thickness Resolution	Relevance to Natural Structure Imitation
Directed Energy Deposition (Metals and Metal-Ceramic Composites)	Laser/e-beam melts powder or wire onto a metallic substrate.	> 200µm	Creating functionally graded materials and structures. Coatings and surface modifications. Used for large, part scale, components.
Powder Bed Fusion (Metals, Ceramics, and Polymers)	Laser or electron beam selectively fuses regions of a powder bed.	> 30µm	High definition features (typically single material). Ideal for smaller scale components requiring significant starting material.
Material Extrusion (Ceramics, Polymers, and Bioinks)	Material is dispensed through a nozzle	> 100µm	Continuous or discontinuous polymer-ceramic composites with low overall feature resolution.
Vat Polymerization (Stereolitography) (Polymers and Polymer/Ceramic Composites)	Photopolymer is selectively cured by light activation polymerization	> 15µm	Discontinuously reinforced polymer-ceramic composites, high resolution features in polymer-based components.
Material Jetting (Polymers and Composites)	Droplets of build material (i.e. photopolymer or thermoplastic materials) are selectively deposited	> 15µm	Polymer-based multi-material components using hard and soft phases. Can also be used for multi-color components. Ease of changing feedstock from one photopolymer to another.

2.1 Nacre-inspired structural designs: A prime example of a structurally and compositionally graded material that has been mimicked via 3D Printing is the nacre shell (see **Figure 3A**) [17–22]. Sometimes referred to as "mother of pearl," nacre is a natural structure mainly composed of aragonite that is a polymorph of calcium carbonate, $CaCO_3$, arranged in a brick-and-mortar like structure with nanometer-scale platelets, whose orientation(s) are governed by the surrounding organic network. Nacre shell's natural growth in bivalves, gastropods, and cephalopods consists of several layers forming a growth-front with subsequent layers growing sequentially due to nucleation from a rich organic ring that forms around the existing tablets, resulting in sometimes 3-4 overall layers formed per day [23]. This structure is of significant interest to the materials community because the mineral bridges serve as a "cement" to enable

plastic deformation and transfer of load between aragonite mineral platelets, enabling a strong yet tough microstructure exhibits outstanding crack-arrest capability. Because these structures maintain both composition and structural variation, mimicking is mostly accomplished via deposition based processes such as fused deposition modeling, direct ink writing, or material-jetting based processing (see **Table 1**).

Fused deposition modeling and direct-ink-writing are used with thermoplastic polymers, inks, and gels, respectively, and are known for the ease of use and a wide selection of materials (see **Fig. 4A and 4B**) [24]. The main mechanism for FDM building is thermoplastic filament extruded through a heated nozzle, controlled at the polymer softening temperature, typically between 100 and 250ºC depending on the polymer chemistry. After extrusion, the filament is cooled on the build substrate and/or previously deposited layer via combined conduction through the substrate and convective heat transfer via a fan and solidified to form the current layer. Complex designs, as is often the case with Nature-inspired structures, require supporting material to be extruded through a separate nozzle before the print-material is deposited, providing structural assistance for the next layer, primarily in locations with features such as internal porosity, steep overhangs from the base material, or other small-scale features. The supporting material can either be the same as the printed material or a dissolvable material that can be removed later using solvent and/or warm water. Parameters that govern these parts' characteristics are the layer-by-layer deposition orientation relative to the build plate, layer thickness, air gap "hatching" distance between raster-paths, width of deposition, and extrusion head temperature, among others [25]. In general, parts with larger layer thicknesses such as ~200 to 400µm lead to lower tolerancing capability than lower layer thickness, particularly in changing cross-section areas from layer to layer [26]. For naturally-inspired structures, material

compatibility can arise with the deposition of multiple materials in tight locations, namely coefficient of thermal expansion (CTE) mismatch and immiscibility, which can lead to stress-induced cracking during processing as well as weak and/or deteriorated properties in the as-printed condition, depending on the nature of the exact additive process used during fabrication. Because FDM is a thermal process, cyclic heating and reheating can lead to delamination between subsequent materials and/or the connection to the build-plate, resulting in challenges with repeatability and quality in the final as-printed structure. Annealing heat treatments are often performed on the as-printed parts to reduce thermal residual stress and compress air pockets between layers to increase strength and rigidity, which poses a significant challenge for working with multiple materials of different properties and characteristics. Direct-ink-writing is a similar overall process, but inks are utilized instead of filament, and complex interactions between material viscosity, nozzle size, and environment play a significant role in the resulting processability and properties. Material jetting (or MJ, see **Fig. 4C**) utilizes the deposition of thermoset polymers on a build substrate, typically a single material, but sometimes one material for the structure and the other for support, as well as one material used for matrix and the other for reinforcement in the case of composites structures mimicking natural materials [24–27]. The material jetting process mechanics involve the viscous-liquid monomer's direct jetting, as specified in the slice file. After the layer is finished depositing, a UV light is exposed to the entire build area or continuously exposes the build material immediately after deposition, curing the monomer. Liquid viscosity plays a critical role and is the main reason why HP™ has become such a large player in machine manufacturing for this process due to its rich history in droplet-based printing technology. Because it is a deposition-based process, multi-material and multi-color parts are easily implemented by a change of deposition material, and in the case of natural-structure imitation, matrix, and reinforcing phase [18]. Additional variations of material jetting

have emerged from the desire to combine the best aspects of several different processes. One example of this concept is Polyjet technology, created to combine high-resolution capability with multi-material and/or color possibilities in a single part. This process employs a liquid-resin jetting head, which uses multiple nozzles to deposit different polymeric materials onto a substrate for a single layer. These materials can be different resins entirely or a combination of support material and the actual build material. Like standard material jetting, after each layer has been deposited, a UV light comes across the surface to cure the deposited liquid resin. This technique is known for combining high-resolution features without requiring large resin amounts such as stereolithography or SLA technology. This process is optimized for small-scale (<~5in

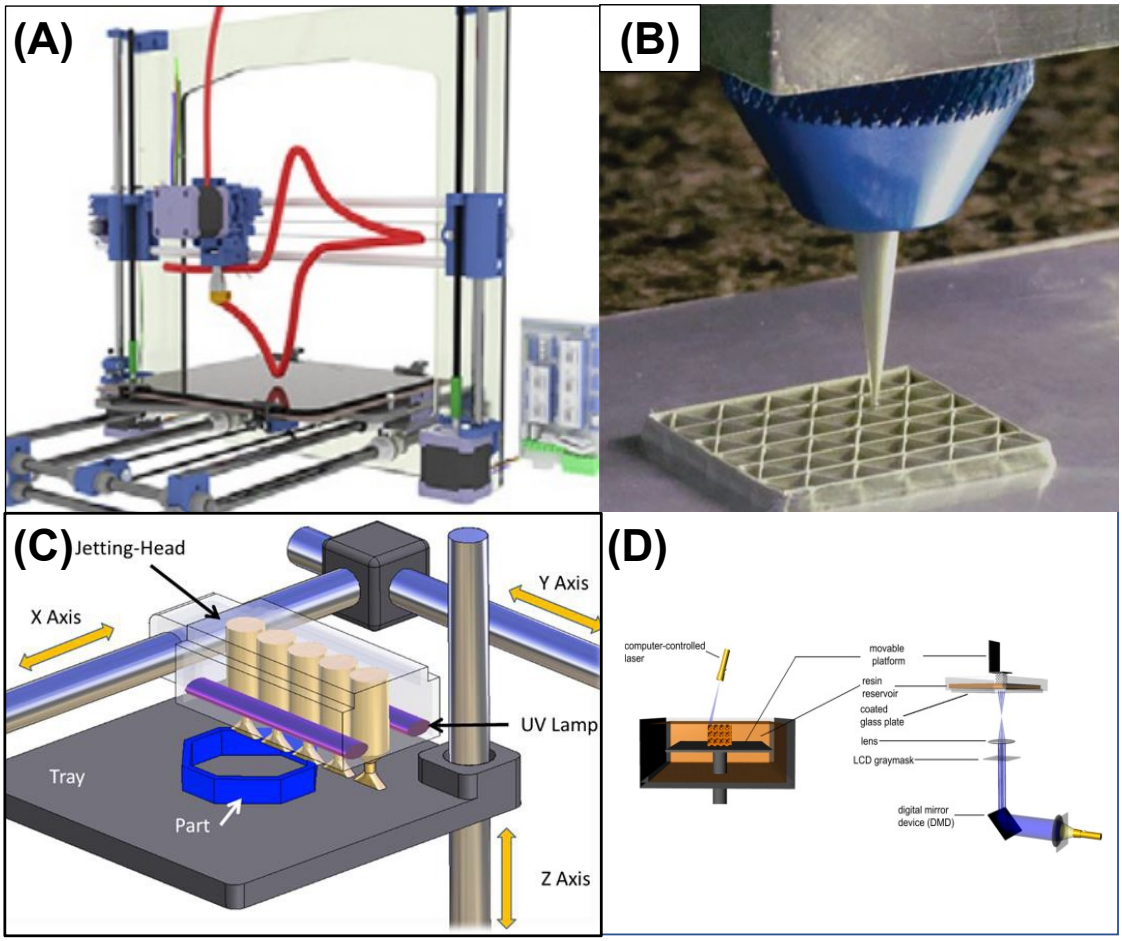

Figure 4: Naturally-inspired polymer-based manufacturing approaches using additive manufacturing. **(A)** Fused deposition modeling (FDM) [130]. **(B)** Direct ink-writing (variant of FDM) [106]. **(C)** Material jetting (PolyJet) [131]. **(D)** Stereolithography (SLA) [36]. Buildplate sizes ranging from centimeters to, sometimes, several meters in size depending on manufacturer.

square) components, as SLA can produce larger components in much less time due to the mirroring functionality that enables fast production. Another related technology is Multijet Fusion, an AM technique originating from HP (Palo Alto, CA) that combines material jetting with binder jetting to create multi-color and higher resolution parts than is achieved using selective laser sintering, SLS. Similar to the binder jetting process, described further detail in ref. [28,29], a layer of material is drawn across a powder bed, and a binder is deposited in a designed manner to create a layer. This process's key aspect is the combination of liquid binder and "detailing" fluid deposited around edges of tight-tolerance requirements. The "detailing" fluid ensures that particles near the edge are not bound to the current layer, creating a smoother final surface finish and tighter overall tolerance for parts produced. While this technology is still evolving, it has seen significant interest from the public to develop multi-color and visually-pleasing components. Some of the main challenges with this process, particularly for nature-inspired structures, are mixing materials during processing, resulting in processing inconsistency when working with multiple materials and reduced tolerancing capabilities. Optimization of feedstock aspects such as particle size distribution, surface energy, chemistry, etc. relevant to the process is critical, especially when attempting to construct multi-material components. While the powder-bed based methods are typically known for creating monolithic components, incorporating powder mixtures instead of single powder lots, as well as varying the processing parameters during a print, can lead to structures with variable phase and chemical composition along the build direction, but with the added challenge of optimizing parameters for multiple different materials that may pose powder cohesion, phase stability, and overall processing reliability challenges due to the different nature of the materials.

Many works have used these methods combined with the nacre as an inspiration for developing composite structures with improved toughness and strength compared to the base constituents. Gu et al. (2017) utilized material jetting to study synthetic nacre on the macro-scale [30]. By utilizing two different photopolymers, one stiff and the other compliant, complex architectures were fabricated with and without connectors, i.e., "mineral bridges" between the larger platelets. By varying the overall platelet vol% from 50-90%, the authors found that the mineral bridges, one of the critical aspects unique to the nacre shell, tended to positively affect the strength, toughness, and stiffness, without providing a detriment to one exclusively. A visual of the overall volume fraction of platelets and mineral bridges are shown in **Fig. 3B**, whereby variable volume fractions of a stiff matrix are devised by variable dimension "unit cells," or repeated units that comprise the overall structure, with "mineral bridges" that join segregated regions of platelets and provide additional reinforcement. While natural nacre maintains roughly 90to 95volume% platelets, the authors found that the naturally-inspired, synthetic design of 80 vol% platelet with mineral bridges exhibited the best combination of properties [30]. The mineral bridges tended to tailor the deformation from variable bulk/reinforcement into a more bulk-type deformation with a single failure point and limited crack deflection, indicating that the unique designs made possible with the additive manufacturing method can very easily affect how a structure deforms under load. In related work, Dimas et al. (2013) explored the use of material jetting to fabricate bio-like cementitious composites with multi-material architectures of varying structural design and material composition [31]. As high as a 20-fold increase in toughness was demonstrated compared to the constituent photopolymers, owing exclusively to the 20wt% compliant phase arrangement stitched between the stiffer phase. Because of the material-jetting process, strong interfaces were formed between the phases, and the deformation was primarily initiated within the compliant phase, indicating that this fabrication approach may be possible to

create damage-tolerant structures in a single processing step, whereby two separate photopolymers are deposited on a substrate and subsequently cured via UV light after each successive layer. **Fig 3C** portrays a comparison of the experimental and simulation results for the brick and mortar structure, indicating that strong agreement between the model and the simulation exists for understanding the crack arrest within the compliant phase [31]. The crack tip is blunted significantly before further crack propagation out to the boundary due to load eccentricity under higher strain. In related work, Tran et al. (2017) utilized the concept of Voronoi diagrams to generate a nacre-like model that was subsequently printed using the FDM technique [32]. A combined design-finite element analysis-experimentation workflow showed that shear failure between the platelet-bridge interface could be a determining factor in the failure of the nacreous structures. High strain rate analysis showed that plastic damage could be mitigated due to the structures' cohesive and incohesive bonding. Interestingly, it was noted that after loading, the different layers within the bulk structure undergo variable amounts of deformation under loading, with the outer layers exhibiting significantly higher plastic deformation. A summary of additional works is provided in **Table 2**.

Table 2: Summary table of additive manufacturing of nacre-inspired structures.

Ref.	Process and Material(s)	Design	Unique Performance and/or Processing Advantage
Gu et al. (2017) [30]	Material jetting, acrylic photopolymers	Variable volume fraction of stiff platelets: 50-90%	-Synthetic mineral bridges along stiff platelets tend to increase strength up to 80% platelet vol% -80 vol% stiff platelet composition exhibited the best combination of strength, stiffness, and toughness compared to others.
Tran et al. (2017) [32]	Fused Deposition Modeling, ABS/PLA panels	Voronoi reinforcement designs emblematic of nacre panels	-Models demonstrated that shear failure is the dominant failure mode under tension due to relative sliding between the laminates. -Plastic damage under high strain rate loading can be mitigated owing to the combination of cohesive and incohesive bonding in nacre designs.
Dimas et al. (2013) [31]	Material jetting, acrylic photopolymer(s)	20 vol% compliant phase, fabricated in bone-like, rotated bone-like, and bio-calcite configurations	-Constituent materials exhibit brittle response individually but high toughness when combined hierarchically -Deformation ensues within compliant material, not between compliant-stiff interface -Multi-scale modeling demonstrated good agreement with experiment for all but bio-calcite configuration-
Yang et al. (2019) [33]	Electrically-assisted Stereolithography	Aligned ~25nm graphene nanoplatelets act as reinforcement within a photopolymer.	-Graphene nanoplatelets significantly enhance the toughness and strength of the photopolymer. -Electrical alignment of the nanotubes leads to sensing capability due to disturbance in the electrical signal transmitted through the platelets.
Liu et al. (2020) [22]	Material jetting, photopolymers	Variable "waviness" angles (±10°) between adjacent unit cells, volume fraction platelets (50-90%)	-Design of an interlocking mechanism between platelets significantly increases strength under tension relative to a flat plate design. -Under tensile load, increased toughness was governed by multiple factors that increased load distribution and limited the chance for platelet cracking under low loading.
Traxel et al. (2020) [34]	Alternating-material based directed energy deposition	200-250µm hard NbC ceramic regions with a bulk titanium structure	-Regions of metal and metal-ceramic composite were processed via modified DED -As high as 40% difference in elastic modulus and a 15% difference in thermal diffusivity achieved with

Other works have used the nacre concept as inspiration to look at existing processes in unique ways, often modifying standard AM techniques such as stereolithography and metal-AM methods directed energy deposition (DED) and powder bed fusion (PBF). Stereolithography (SLA), the original AM process [35], is governed by the movement of a UV light across the top surface of a monomer vat, outlining a pattern determined from the slice file (see **Fig. 4D**) [36–

41]. In this variation, laser curing occurs starting from the top of the vat, with the build platform moving downwards to create additional layers. After many layers are completed, a component is produced, and the part can be removed from the build plate. Complex functionality can be incorporated into the component by tight control of the thickness of the features within each layer, i.e., thin sections can form a strut that is cured and support other features like overhangs in the as-printed structure and can be removed after Printing. Such capabilities make SLA a common technique for fabricating functional parts and "fit-check" prototype components for different applications. Enhanced systems use a "flood" light, allowing multiple areas to be scanned at once, thereby significantly increasing throughput in production environments. The main challenge with this technique is multi-material processing because the vat must be filled with the build material, and to change materials, the whole vat must be emptied. Despite this fact, SLA machines are widespread in the industry, and as such, variations can utilize a ceramic or reinforcing phase mixed in with the monomer bath, resulting in a composite material with enhanced properties [42]. The main AM methods (with some modification) commonly utilized in the fabrication of naturally-inspired structures for metallic-based materials are directed-energy-deposition (DED) and powder-bed-fusion (PBF), owing to their combination of multi-material capability and high-resolution feature creation, respectively [43]. Both PBF and DED techniques utilize a laser or electron beam to fuse metal powders or wire in a layer-by-layer manner (see **Figure 5A & 5B**). The main difference between the techniques is that DED makes use of a powder flow/wire feedstock to deposit material onto the build substrate, whereas in the case of PBF, the powder is already within the build chamber, and the energy source need only trace out each new layer [44,45]. On each layer, a roller is used to transport a thin layer of powder across the top surface from the compacted powder reservoir onto the powder bed surface, as shown schematically in **Fig. 4B**. The build side will drop to a slightly lower height than the next layer

thickness, where the roller subsequently compacts the next layer of powder down onto the substrate by rolling back over to the build side. At this point, a concentrated high-power laser with a focal point at the build surface rasters along the surface, outlining the cross-section shape at the given layer, shown in **Fig. 5B**. Examples of end-use components include carefully-designed porous implant materials [46–49], complex internal features and channels [50,51], high-performance coatings [52–54], functionally and compositionally-graded structures [55–58], component repair [59–62], among many others. One of these processes' main challenges is the presence of inconsistencies in the as-printed microstructure, defects, and porosity and warping [44,63–65]. Several phenomena such as pores, balling, and the "keyhole effect" occur when too high power is used at low scan speeds, and the heat source can penetrate material [64,66,67]. Microstructural and mesoscale modeling has been investigated to model phenomena such as grain growth, phase formations, and other defect mitigation approaches to decrease the experimentation burden on manufacturers [68,69]. Additional integrated approaches have been made to combine different length-scale simulations and experimental data to explain such phenomena [70,71]. Several variant strategies have been utilized to create advanced composites relevant to the multi-material architectures found in Nature, namely, *in situ* processing strategies such as nitridation [53,72], reactive-deposition [73,74], or ceramic-phase deposition and reinforcement [75,76]. These methods have laid the groundwork for developing manufacturing frameworks and materials to mimic natural structures such as the nacre shell.

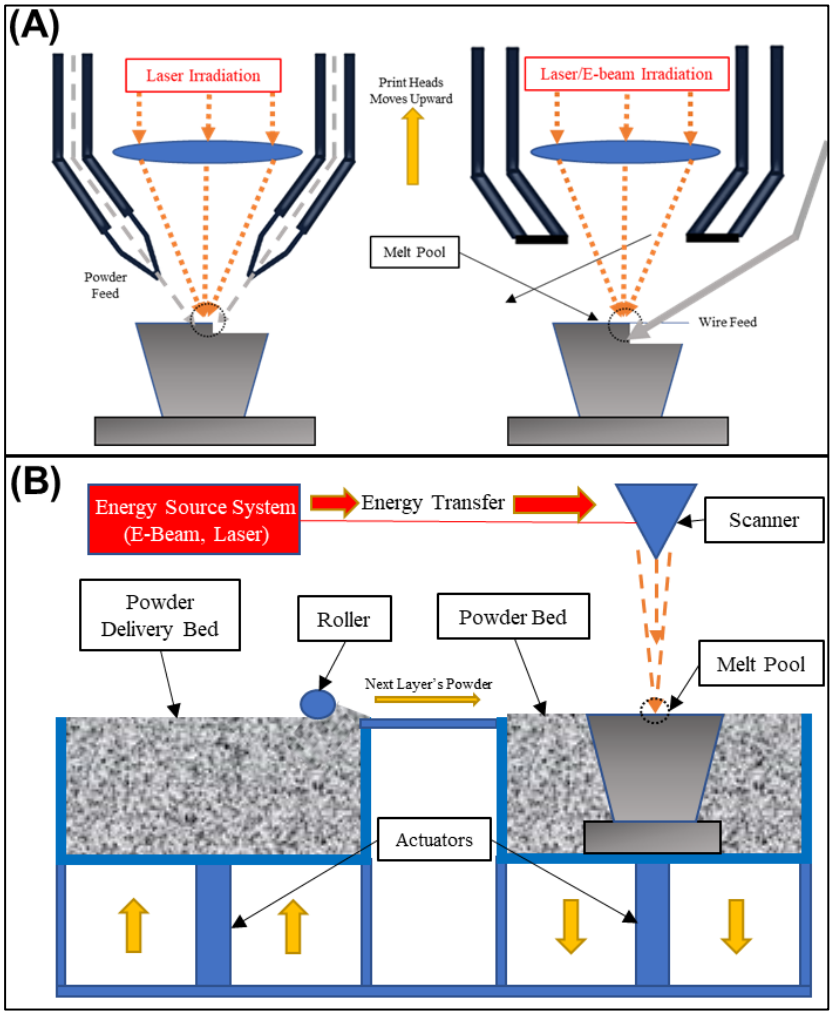

Figure 5: Naturally-inspired metallic-based manufacturing approaches using additive manufacturing. **(A)** Directed energy deposition. **(B)** Powder bed fusion. Both images from ref. [13]. Build plates are typically on the order of several hundred millimeters, and in some cases, meters depending on the manufacturer.

Mirzaali et al. (2019) recently demonstrated an FGM process via a material jetting approach [77] that involved variable composition from soft to hard photopolymer in stepwise as well as continuous distribution along the length of the build [77]. Yang et al. (2019) utilized an electrically-modified stereolithography technique to create nanoplatelet graphene reinforced polymer structures [33]. As shown in **Fig. 6A**, the applied electric field enables the nanoplatelets to be aligned, resulting in a brick-and-mortar type structure emblematic of the nacre. Although this process is typically thought to be used for single-material components due to the large vat of material, the authors successfully process a composite composition within the vat. Control of the homogeneity of the reinforcement graphene phase is a challenge with this process, but the authors reported similar overall fracture paths in the 3D-Printed specimen in comparison to actual nacre under similar testing conditions,

indicating that these composites have unique and desirable behavior under loading. The electrically conductive platelets' presence led to the ability to sense when the structure was under deformation, providing insights into futuristic multi-functional structures that can provide *in situ* diagnostics into internal failures. In another work involving metallic structures, Traxel et al. (2020) explored the use of DED-based technology to emulate the soft, hard reinforcement found in natural structural materials (see **Fig. 6B**) [34]. Although this process is traditionally thought to be used in applications requiring repair or developing functionally graded materials, the authors envisioned producing a ribbon-like structure capable of directional-thermomechanical performance. By alternating titanium and niobium carbide deposition, the authors reported distinct metallic and metal-ceramic composite (~40-75% ceramic composition) that exhibit directionally dependent properties. As high as 40% difference in compressive stiffness and 31% difference in thermal diffusivity were exhibited and significantly different properties compared to a composite of premixed composition with similar overall reinforcement value. Shown in **Fig. 6B**, this composite exhibited unique crack-arrest capability within the reinforcement region that contributed to strengthening and directionally-dependent performance, indicating that the directed energy deposition process can be customized to create structures that can withstand directionally-dependent loading environments.

From a processing perspective, most of these works commented on the challenges of creating a multi-material architected structure with strong, cohesive bonding between the hard and soft phases and how that affects the build quality and the properties of the macroscale composites. In many cases, these challenges are process and material-system specific. More specifically, nacre's features exist at the nanoscale, which is a size range that is still out of reach for most 3D-printer technologies, motivated engineers and researchers to push the limits of the printers, which likely leads to inaccuracies or discrepancies in the quality. This aspect is further accentuated when depositing

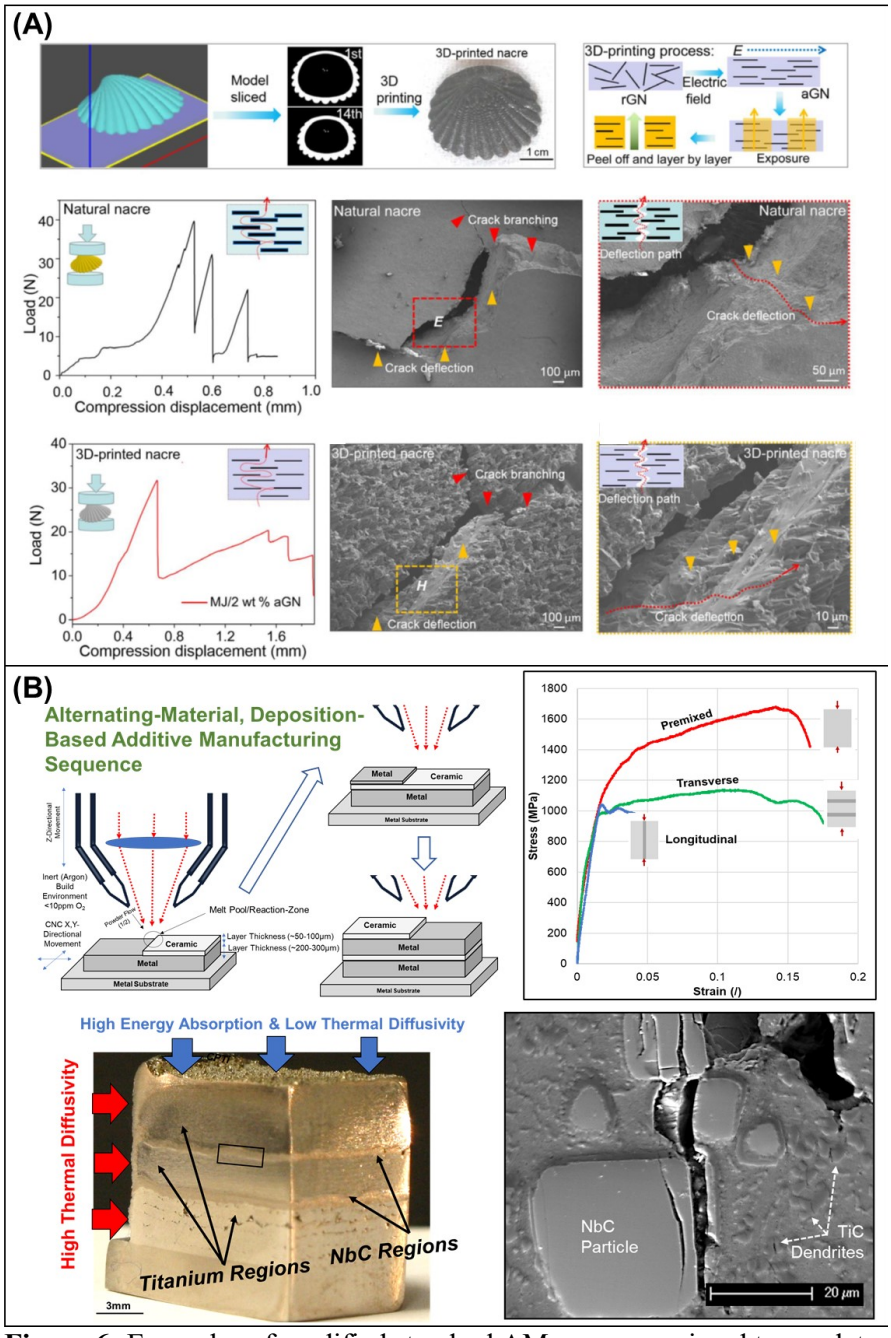

Figure 6: Examples of modified standard AM processes aimed to emulate nacreous composites. **(A)** Electrically-assisted SLA processing, adapted from [33]. **(B)** Alternating-material deposition additive manufacturing based on directed energy deposition process [34].

multiple materials in very small locations to provide site-specific properties. More specifically, it was noted in the work of Dimas et al. (2013) that inaccuracies due to mixing at the interface of the soft and hard phases during material jetting caused discrepancies in the accuracy of the simulation in providing insight into the experimental results (>50% difference in the effective yield strength) [31]. Additionally, Frelich et al. (2017) reported that the mineral bridges themselves (when processed via material jetting) tended to result in circular cross-section as opposed to prismatic, owing to the Nature of the droplet-like process to produce rounded structures at smaller scales [17]. These discrepancies likely led to decreased load transmission through the mineral bridges, resulting in much lower toughness values at smaller bridge dimensions. In the work of Traxel et al. (2020), as well as with most laser-based processes, residual stress and cracking can occur due to the differences in the CTEs of the materials and high thermal gradients within the process, providing significant challenge from a reliability standpoint in processing [34]. Because of the complex multi-material aspects of the process, each material combination requires extensive processing optimization through parameterization studies, testing, and characterization to understand the damage mechanisms and feedback to the structures' overall design. These aspects highlight the importance of design considerations for nacre-like structures at smaller length scales and the overall difficulty of producing such structures. It is envisioned that with machine component improvements (higher resolution scanning laser systems), simulation software for residual stress prediction and final part properties, and additional studies published, we can develop an improved understanding of how such multi-material structures can be fabricated in reliable ways.

2.2 Bone-like structural designs: Another exemplary natural structure that is increasingly emulated via additive manufacturing is human bone [49]. Bone is a complex structure with variable porosity and composition from the inside to the outside, changing over time in a person's life due to age, activity level, and sometimes disease (osteoporosis, osteosarcoma, among others) [78,79]. In different areas, the calcium phosphate-collagen composite must withstand variable stresses, particularly in the hip joint, as shown in **Fig. 7A**. From a design perspective, healthy bone's unique damage tolerance originates from intrinsic toughening

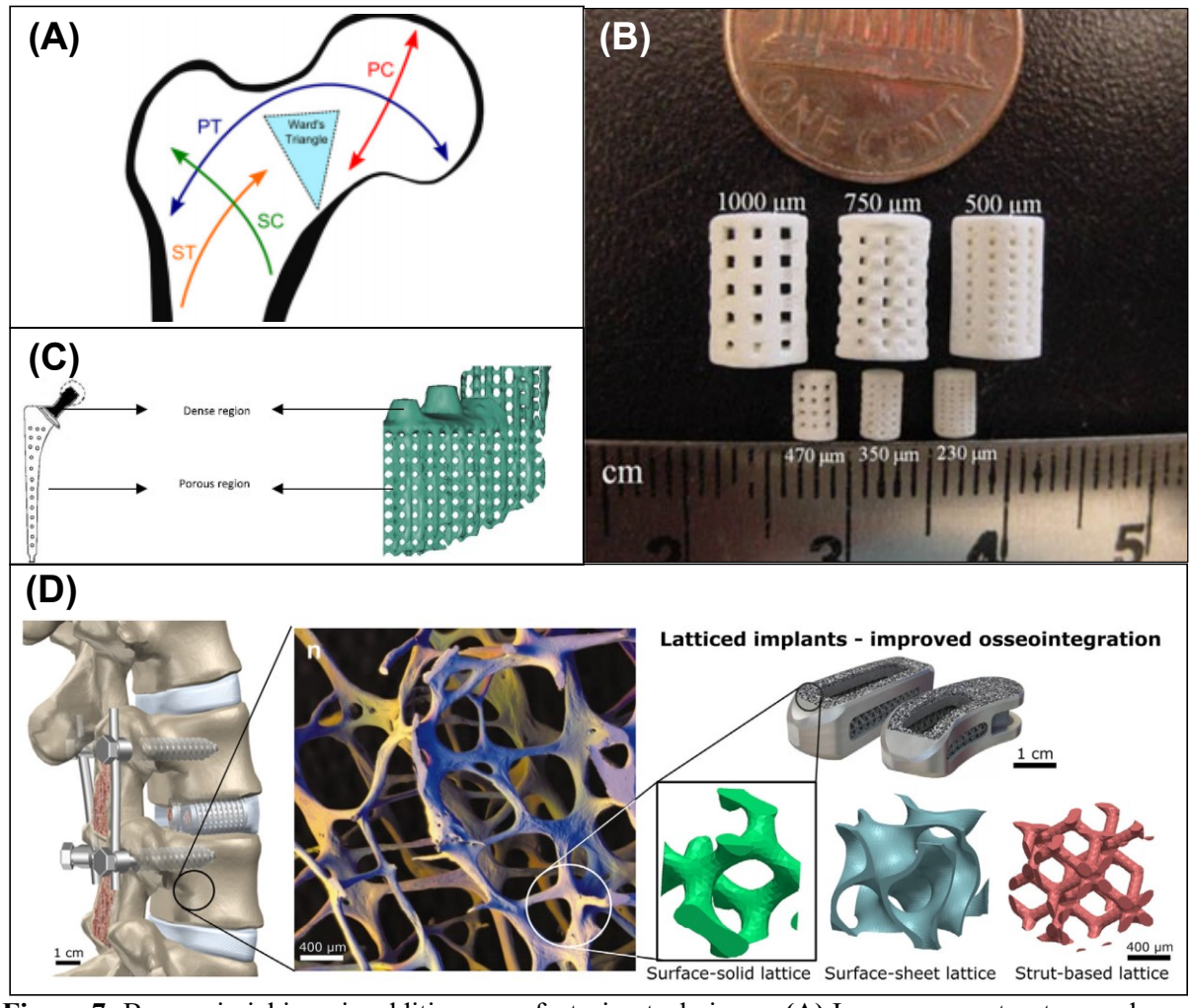

Figure 7: Bone-mimicking via additive manufacturing techniques. **(A)** Inner porous structure and specific principle and secondary compressive/tensile loads exhibited by a healthy hip joint (P/S and T/C corresponding to Primary/Secondary Tensile/Compressive stresses) [128]. **(B)** Bone structure and composition matching via controlled porosity in calcium phosphate scaffolds manufactured using binder jetting [80]. **(C)** Hip stem porosity and mechanical property matching via CAD [81]. **(D)** Spinal joint lattice optimization for controlled porosity and increased osseointegration [78].

generated by the allowed plastic deformation of fibrils that slide against one another between mineral platelets, enabling the load to be transferred from one platelet to another while resisting complete failure [3]. Additionally, the internally graded-architecture from both structure and composition perspectives enables efficient load transfer and biological function, making it desirable as a design concept in structural applications. For biological purposes, the cancellous inner portion of the bone provides porous areas of high vascularization, and the cortical outer portion provides lower porosity, high stiffness, and extrinsic crack deflection/twist capability to avoid fracture, resulting in an overall tough composite material [1]. The complex, functionally-graded Nature of bone is difficult to emulate using traditional manufacturing techniques, which has motivated significant investigation into additive-based processing methods that can combine producing complex features in small locations with variable composition in single components. In addition to emulating bone's unique structural qualities, significant motivation has come from the field of tissue engineering, where patient-specific implants with desired properties are required [47,78,80–82]. More specifically, researchers have investigated additive manufacturing to produce implant materials with similar properties to the bone to alleviate stress-shielding complications, among other challenges in biomedical applications.

Like nacreous-structure mimicking, bone-emulation has been accomplished via several additive manufacturing methods. Tarafder et al. (2013) utilized the binder jetting method to fabricate tricalcium phosphate scaffolds with designed porosity to reach specific mechanical properties and structural characteristics close to bone [80]. Although binder jetting has historically been used for metallic materials, process parameters such as layer thickness, binder droplet volume, saturation, and roller spread, among others, were adapted to work with ceramic materials with a similar composition to bone (calcium phosphate). In this work, pore sizes were

designed from 230-1000μm, and microwave sintering post-processing (see **Fig. 7B**) significantly increased the scaffolds' mechanical strength due to volumetric heating and lower overall internal porosity. This resulted in comparable scaffold mechanical strength to cortical bone, indicating their efficacy in bone-tissue engineering applications. Similar work by the same authors has been accomplished with other calcium-phosphate composites with additional drug loading for further efficacy in different bone-tissue engineering applications [83–85]. In other works, metal-based materials have been investigated to apply bone tissue engineering applications through site-specific porosity control (see **Fig. 7C**) [46,81,86–94]. Most of these works' goal is not to directly mimic the structure of bone but rather to leverage additive manufacturing to create scaffolding structures that maintain similar overall properties compared to bone. Barba et al. (2019) utilized powder-bed-fusion (PBF) to fabricate samples comprised of what are referred to as "triply periodic minimal surfaces," or TPMS, to match the properties and mechanical response of bone (see **Fig. 7D**) [78]. Four different lattice archetypes were used, with distinctly different mechanical responses and different porosity levels (15-85%). Varying the porosity allowed the scaffolds to decrease in strength to roughly the strength of bone, and optimized pore diameters were shown to be in the range of 300-600μm. In similar work, Parthasarathy et al. (2011) demonstrated the ability to tailor a scaffold's structure using structural finite element analysis (FEA) software [81]. By editing the computer-aided design (CAD) of the scaffold itself, the properties of the overall structure were predicted, and then the Printing of the structures was performed to compare the computer model to the actual properties of the structures. Their reported results indicated good agreement with the computed properties of the structures. A summary of additional works is provided in **Table 3**.

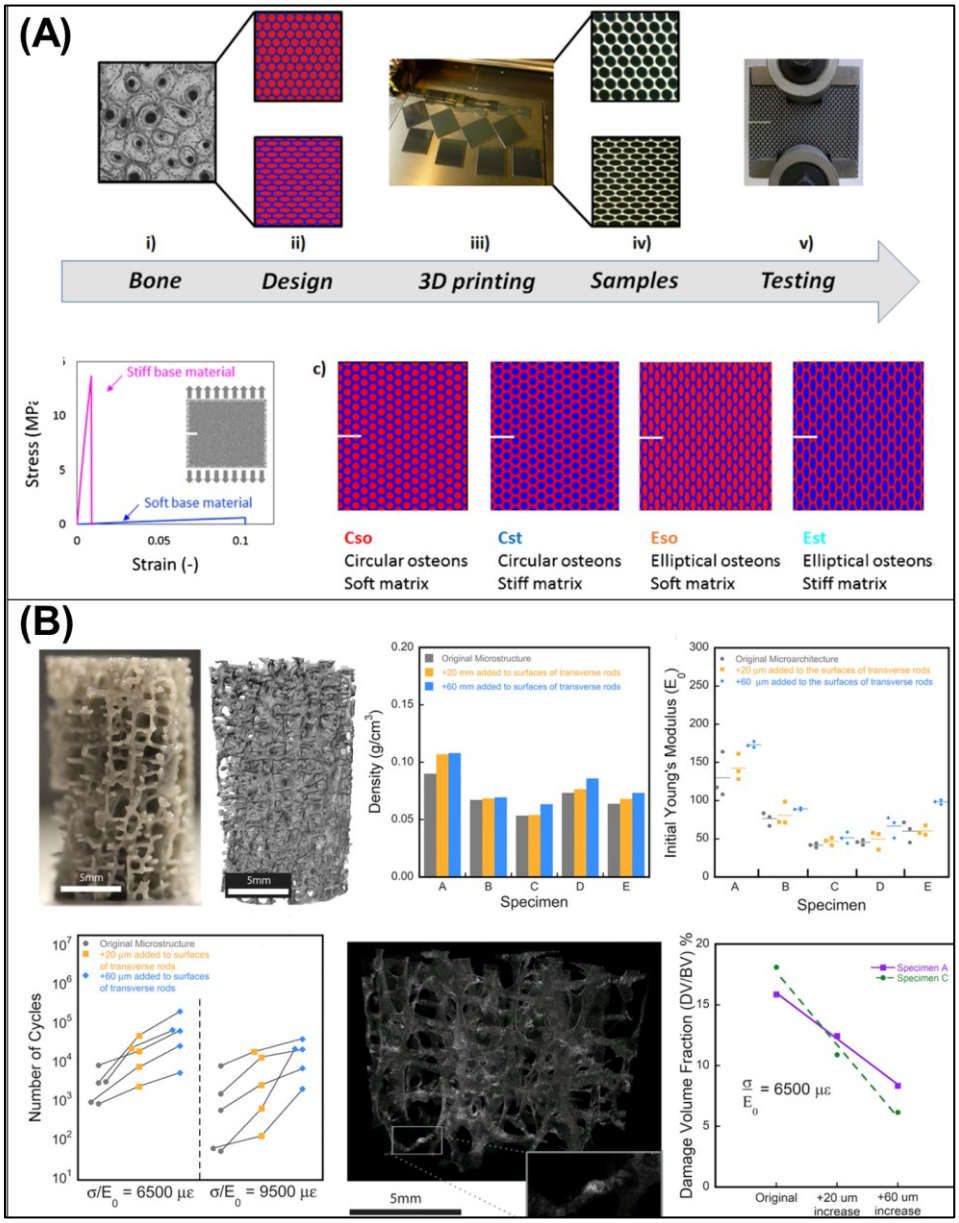

Figure 8: Properties of bone-mimicked structures created via 3D-Printing. **(A)** Design of bone-inspired composites with variable soft/stiff matrix as well as cylindrical/elliptical reinforcement, manufactured using PolyJet processing as 80mm square samples of 3mm thickness [95]. **(B)** Fatigue performance of variable-strut size lattice composites recreated from bone and processed using stereolithography [96]

Other authors have tried to reverse-engineer and, sometimes, recreate bone-like structures through AM-based methods. Libonati et al. (2016) explored the mechanisms by which bone amplifies toughness via its hierarchical structure, using the material jetting AM technique [95].

By incorporating soft cylindrical "osteons" within a hard polymer matrix, similar to bone, the authors were able to test the directional response to different loading conditions commonly observed in bone, as well as the effects of different combinations of soft/stiff matrix and

circular/cylindrical osteon design (see **Fig. 8A**). Interestingly, the composites exhibit toughening mechanisms similar to bone, namely, fibril bridging, microcracking, and crack deflection/twist, which all contribute to the structure's toughening under tensile load in comparison to the base constituent materials. The elliptical inclusion design led to more crack branching than the circular inclusions, which led to more crack deviation, indicating that the elliptic case results in a tougher overall structure. In another study, Torres et al. (2019) investigated the fatigue behavior of bone-like architectures using SLA based additive manufacturing (see **Fig. 8B**) [96]. Because most works have been focused on merely the strength of scaffolds, fatigue properties have been largely overlooked for lattice-based structures. The authors based their designs on computer-tomography images of human cancellous bone, with modifications made to the strut size to see the influence on fatigue behavior. The authors reported significantly improved fatigue life with increased strut size, indicating that internal bone composition and microarchitecture can play a significant role in influencing lattices' mechanical behavior.

From the manufacturing perspective, different investigations have noted challenges in achieving such bone-inspired designs. Barba et al. (2019), which utilized PBF, a minimum strut thickness of 250μm, was mentioned as the lowest resolution with the art equipment state [78]. Some lattice topologies that required special attention to delicate features were reported to be challenging to process in the first place successfully. These are typical challenges for the laser powder-bed processes as the resolution, while thought to be that of the laser spot size (60μm), depends entirely on the class of structure that is attempting to be fabricated. More specifically, while the powder bed is known to act as a slight supporting structure for parts during Printing, the thermal cycling that occurs during processing can account for distortion of components and ultimately build failure should the components distort into the powder-spreading apparatus.

Other polymer-based processes exhibited similar processing challenges, namely mixing hard and soft polymers and dimensional accuracy challenges. These instances demonstrate the challenge to meet the requirements of emulating some of these structures from a design perspective and are essential to note for manufacturers moving forward when developing new systems.

Table 3: Summary table of mimicking the structure and properties of bone using additive manufacturing.

Ref.	Process and Material(s)	Design	Unique Performance and/or Processing Advantage
Libonati et al. (2016) [95]	Material Jetting, acrylic photopolymers	Soft/stiff matrix reinforcement with variable cross section (100–300μm) fibers ("osteons").	-Similar to bone, fibril bridging limits crack growth capability in a stiff matrix configuration. -Elliptic inclusions lead to crack deflection and improved mechanical response.
Barba et al. (2019) [78]	L-PBF Ti6Al4V	Four separate lattice types, 15-85% dense scaffolds	-250μm strut size is minimum for achieving reliable mechanical properties. -300-600μm pore size was shown to be ideal for osseointegration.
Bose et al. (2018) [97]	L-DED Titanium w/surface modifications	200-300μm open pore, 25% overall porosity	Combined porous titanium with surface nanotube modification exhibited
Tarafder et al. (2013) [80]	Binder jetting, tricalcium phosphate	230-1000μm interconnected porosity design	-Microwave sintering results in higher densification and lower overall porosity compared to traditional sintering. -Large interconnected porosity and composition lead to mechanical properties similar to bone.
Hedayat et al. (2018) [98]	L-PBF CoCr & Ti6Al4V	Pore: 310-460μm Strut: 450-876μm Cuboctahedron, Dodecahedron, Diamond	-Different lattice types deformed in different regimes, namely the normalized modulus and yield strength -As high as a 10-fold difference in normalized properties were found with topology change, they were 2-fold with material change.
Zhao et al. (2018) [87]	L-PBF	500,1000μm cell size, Tetrahedron, Octahedron	-Octahedron demonstrated significantly improved load distribution compared to the tetrahedron unit cell, as determined analytically and experimentally. -Higher pore size resulted in improved osseointegration but also decreased mechanical properties.

2.3 Helicoid-like structural designs: Another interesting natural design that has been emulated via additive manufacturing methods are the helicoid, chitinous-reinforcement architectures found in beetles, shrimp, and other crustacean-type creatures [99–105]. **Fig. 9A** shows these materials' constructs, with different regions exhibiting variable laminate angles, which are a predominant factor for such damage tolerance. These structures provide continuous-rotated reinforcement fibers that promote outstanding fracture toughness by adjusting the crack-front interface in the propagation direction [99,100]. For example, in the smashing mantis shrimp, the dactyl club is used as a hammer on prey, generating significant stress waves in the material upon impact while maintaining structural integrity over thousands of impacts. These features have motivated investigations as to the possibility of creating such damage tolerance using additive

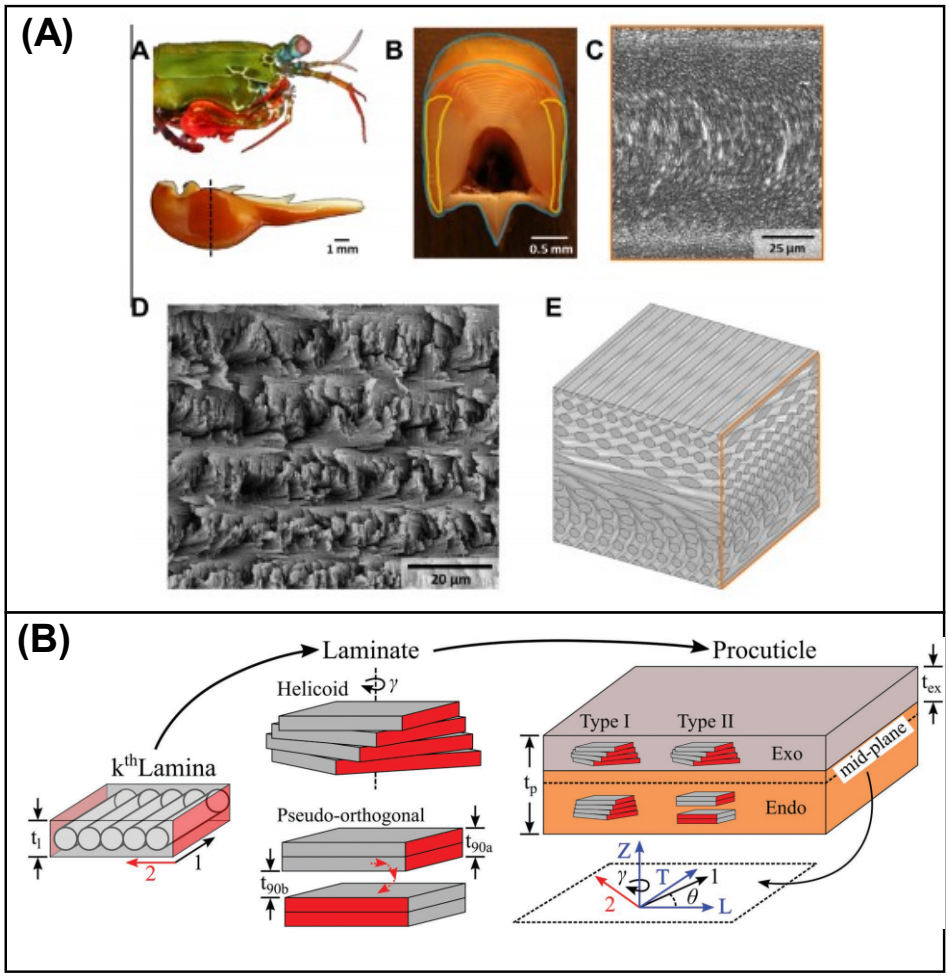

Figure 9: Characteristics and processing strategies of twisted/helicoid natural structures. **(A)** Structural characteristics of helioid structures in a dactyl club of a mantis shrimp [127]. **(B)** Reinforcement strategies for manufacturing helicoid-type structures [99].

manufacturing methods.

Several works have investigated helicoid structure manufacturing via FDM and material jetting processes [99,101]. Zaheri et al. (2018) utilized the material jetting technique to understand the effect of helical angle on the mechanical properties of multi-material (stiff-polymer reinforcement) helicoid composites using both stiff and soft polymers [99]. Imitating the various regions within the shell of a Fig-Eater Beetle, the authors utilized a mechanistic analysis to determine the fiber axis that accurately describes various reinforcement regions and how the stiffness varies within that region (see **Fig. 9B**). Complementary experimental results indicated that the fiber orientation angle profoundly affected these composites' tensile properties. Namely, the elastic modulus tended to increase with the increase in laminate orientation angle, according to laminate composite theory, but divergent from the Krenchel shear-lag theory (modified rule of mixtures). These results showed that the effect of laminate asymmetry carries great importance and the transverse and shear effects within the composites (absent in the Krenchel theory). Another fascinating insight was the strain heterogeneities between different orientation angles, where twisting/torturous fracture surfaces are observed for 15° & 30° orientations, but more brittle fracture observed for the unidirectionally-reinforced laminates. These results indicate that the fracture mechanisms and performance can be altered via adjustment of the helicoidal design's orientation angle and that material jetting can successfully process such structures at structural length-scales.

Additionally, Sun et al. (2020) investigated fiber helicoid-orientation's effect on the tensile properties of Bouligand-like structures [101]. Although only single material (Poly-lactic-acid, PLA) was utilized, the authors recreated four different pitch angles (10°, 15°, 30°, 45°) between layers, which resulted in different overall composites resembling the helicoid structure.

These hatching strategies were compared to standard 0°/90° as well as 45°/45° standard hatching strategies utilized in the literature. Through modeling and experimentation, authors determined that a pitch angle of 15° between subsequent planes creates the toughest and strongest material owing to the increased fracture surface cross-sectional area and lower stress concentration owing to the high fracture deflection and subsequent toughening of the structure, similar to that found in Bouligand structures in Nature.

2.4 Other naturally-inspired structural designs: Other natural structures have garnered recent attention due to their complex architectures and the advance made by using 3D Printing methods. Compton and Lewis (2014) utilized direct-ink-writing (a type of extrusion-based AM using ink-based materials) to manufacture balsa-wood inspired cellular composites to generate lightweight composites with advanced structural performance (see **Fig. 10A**) [106,107]. By incorporating SiC and carbon fiber in their ink-based precursor materials, the shear-thinning phenomena during Printing resulted in preferred alignment and reinforcement in the horizontal printing direction. Square, triangular, and honeycomb lattice structures were manufactured to understand geometry's effect on the resulting mechanical properties. The authors found that fiber-pullout was a significant toughening mechanism in the aligned composites under tension, and properties comparable to balsa wood and highly advanced fiber-reinforced composites could be achieved. While this work was focused on understanding the structural aspects of the composites, Stute et al. (2018) and Correa et al. (2015) have manufactured wood-like structures via FDM and material jetting processes to create complex internal topographies and understand complex hygroscopically-actuated functionality [12,108]. Stute et al. (2018) utilized a custom pixel-to-voxelization process where the authors could take images of the cross-sections of olive

wood and generate a print file to create variable color within a single print [12]. The authors created an alligator structure with the same color texture within this same process, indicating that natural architectures can be embedded into structural components for visual and/or learning purposes.

Another exciting application of natural structural design originates from mimicking metallic crystal structures. Pham et al. (2019) utilized several polymer and metallic-AM processes to study the translation of microscale strengthening/toughening mechanisms on the macro-scale, forming "macro-lattices" (See **Fig. 10B**) [6]. By mimicking face-centered-cubic (FCC) and body-centered cubic (BCC) microstructures via computer-aided design methods, the authors were able to utilize the base unit cells as repeating units in larger structures on the macro-scale (see **Fig. 10B**) and perform various testing and manipulation to the base lattices. Authors utilized PBF-based processing to create 316L stainless lattices containing roughly 8 "meta grains" separated by high angle grain boundaries and achieving yield stress of about 50 MPa, with significant toughening behavior (rising stress-strain curve) under compaction. The authors simulated grain boundary hardening via metallurgical twinning phenomena, precipitation hardening, and multi-phase hardening found in common engineering materials. They showed that, for the most part, macro-lattices could be designed in regards to the micro-scale hardening mechanisms for tailored properties and performance in different situations. While some mimicking of naturally-inspired structures is fairly first-generation and more exemplary than application-specific, these types of lattices have been the subject of significant interest in the biomedical community for direct application. Such "mechanical metamaterials" and "triply minimal surfaces" are emerging as candidates for implant-based materials due to their ability to

combine bone-like moduli, increased biocompatibility and functionality, and lower overall mass densities [49,78,81,109,110].

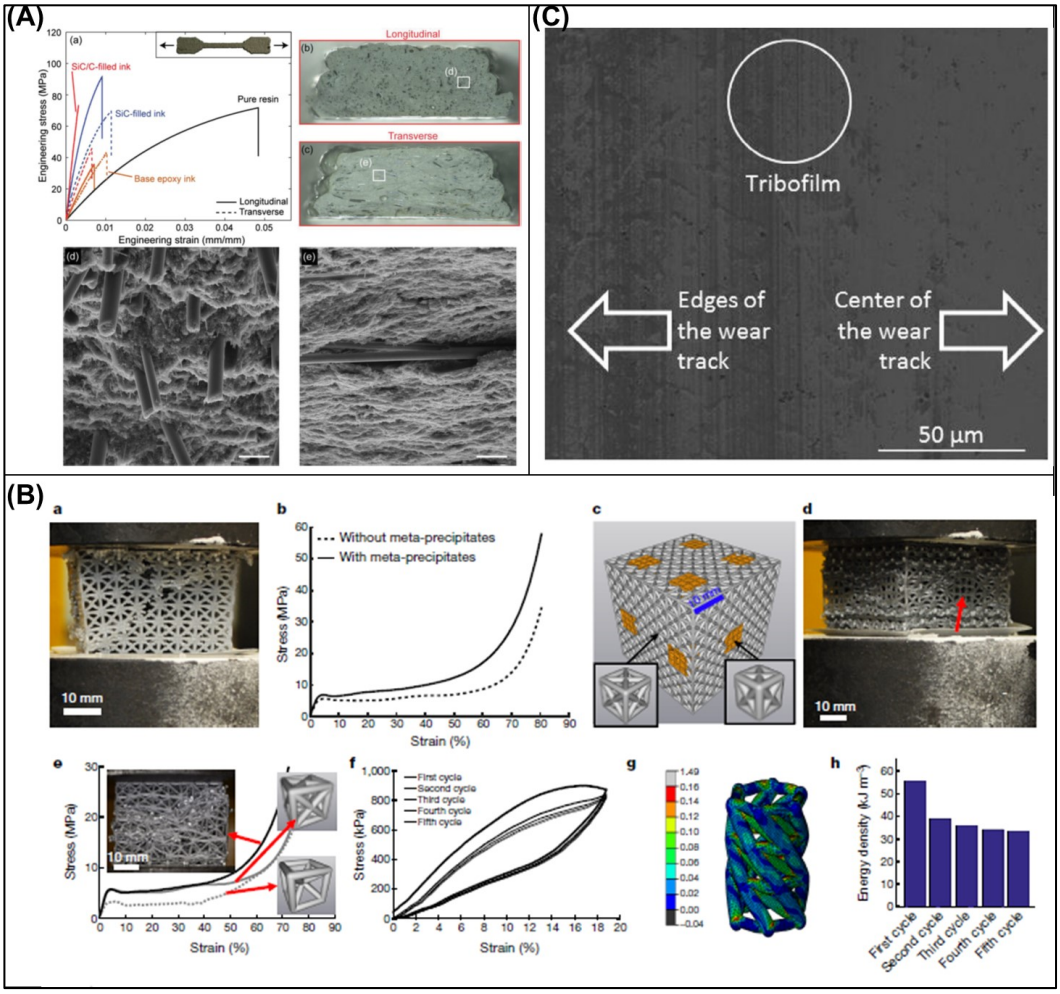

Figure 10: Examples of other nature-inspired structures using additive manufacturing. **(A)** Wood-like composites processed using direct ink writing [106]. **(B)** Metal microstructure-inspired macrolattice structures manufactured using powder-bed-fusion [11]. **(C)** Tribofilm formation in metal-matrix composite coatings for load-bearing knee and hip arthroplasty applications, manufactured using directed energy deposition [76]

Another promising area in the AM community is in the field of self-lubricating surfaces, or manufacturing of lubricious coatings inspired by natural phenomena in reciprocating joints (see **Fig. 10C**). Throughout several works [76,111–114], calcium phosphate-based materials were incorporated into 3D-Printed metal-matrix composite coatings via DED technology to stimulate the wear-resistance of the metallic matrix. While most DED-based coating work for

wear resistance is focused on increased hardness and toughness at the surface level [73,75,115,116], this work has stemmed from the finding that calcium phosphate, either the form of tricalcium phosphate or hydroxyapatite, forms a lubricious "tribofilm" under wear induced phenomena of a metal matrix. It is also increasing the bioactivity of the surface. More specifically, as the metal is contacted and worn down by a reciprocating rubbing action, calcium phosphate that has been premixed with the metallic material will spread along the surface and significantly reduce the material's friction and wear rate as a whole. Sahasrabudhe et al. (2018) demonstrated that as low as 3wt% CaP reinforcement to CoCrMo alloy could significantly reduce the wear rate leeching out of metallic ions in DI water medium [76]. Additionally, Bandyopadhyay et al. (2016) demonstrated similar phenomena in Ti6Al4V, another common engineering material used in knee and hip arthroplasty [112]. These works' primary significance is that metal ion leaching is becoming a huge problem in metal implants for knees and hip arthroplasty. Naturally increasing wear resistance is essential to the modern application while also mimicking friction-reducing phenomena in articulating joints.

3. Current challenges and future direction: next generation of design inspiration

The next generation of naturally-inspired structures leveraged via 3D Printing lies at the intersection of advanced processing and design tools emerging in academia and industry. Two-photon lithography is rapidly changing; among other technologies, researchers view the possible scales involved with additive-based processes [117,118]. Crook et al. (2020) demonstrated nanometer carbon-like structures with strength and stiffness on the outer limits of possibility [117]. Additional work is being done in topology optimization, or the design of structures for AM that are fully optimized for specific loading applications [119–122]. These methods are also

being supplemented by works utilizing machine learning-based methods to improve quality control and the design of structures [123–126]. Such approaches have shown the ability to utilize a closed-loop system on a part design, processing, and end functionality. An example of an advanced workflow concept is shown in **Fig. 11**, whereby a component, in this case, a hip implant, is to be designed with patient-specific properties and useful biological function as a healthy hip. 3D Printing is a great candidate as this component can be patient-specific and combine multiple materials within a single structure or combine separate 3D Printing processes to manufacture such a product. For this specific application, both structure and composition are critical components as they affect the mechanical stiffness, strength, fatigue resistance, and the in vivo bone ingrowth characteristics, resulting in a shorter healing time for the patient. It is envisioned that a metal-based implant could be manufactured via a combination of DED and PBF that combines a fatigue-resistant metallic alloy (perhaps Ti6Al4V or CoCrMo) with lattice structures within specific locations to achieve directional stiffness and strength, and then processed with a subsequent bioactive coating such as hydroxyapatite to stimulate the bone ingrowth at the implant-bone interface. For practical purposes, it may be found that the hip stem may be processed via PBF with a premixed metal-based composition, and the femoral head (upper portion) would be processed separately with a similar overall composition, limiting the need for the subsequent coating. Such design features are the primary considerations for the computer-aided-design and simulation that would be performed to predict the end-use component's performance and the optimal processing parameters. The part(s) would then be ready for Printing and subsequent post-processing through various software and simulation capabilities. Should these parts result in poor quality or performance, a redesign can be undertaken, and if not, they can move on to functional testing and end-use. It is envisioned that such approaches will be made possible with the advancement of current techniques and the

development of next-generation processing technologies based on naturally-occurring structures and materials.

Although there is significant excitement towards naturally-inspired structures, challenges

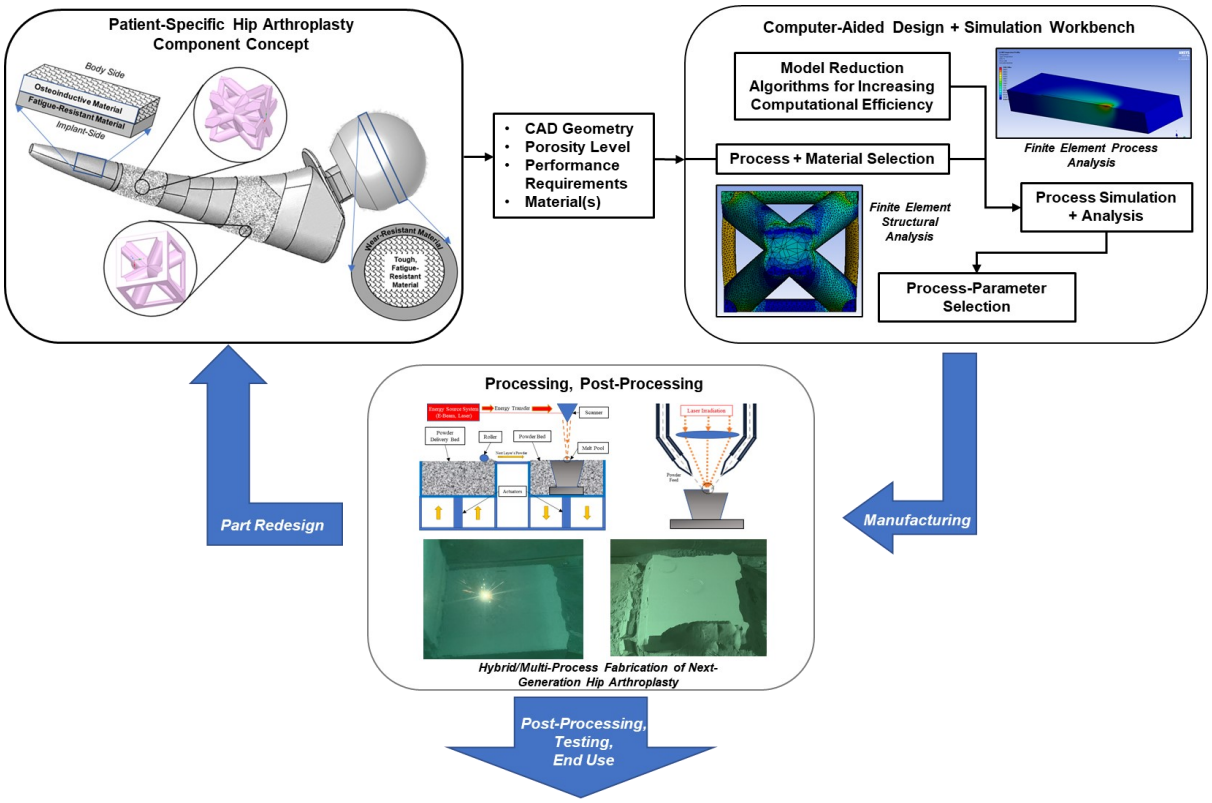

Figure 11: Process workflow concept for incorporation of composition and structural variation into structural components utilizing additive manufacturing.

still exist in design issues and 3D printing processes, particularly when developing multi-material structures with complex features. Design of multi-material structures via CAD with functional properties that can be sliced with different slice thickness based on materials or part complexity, and create different tool-path for different regions are still difficult. Much of this challenge can be alleviated with the development of design software that can incorporate thermal/structural analysis that can help engineers understand the critical relationships between component design (both bulk properties and reinforcement properties), specific processing aspects related to thermal/structural cycling, and overall component properties after processing.

For example, understanding the relationship between reinforcement alignment and overall amount within structures imitating bone, nacre, and/or Bouligand structures. Moreover, most AM platforms are designed for one type of material such as metal or plastic, and manufacturing different materials in the same operation with very different properties are still challenging, and in many cases, not possible. This motivates hybrid manufacturing strategies and new 3D Printing platforms from which researchers can benefit. Despite the attention paid towards some of these challenges posed by the emulation of naturally-inspired structures, it is essential to note that researchers and designers have significantly advanced the state of the technology in recent years. While most published works have focused solely on the front-end design or different manufacturing aspects of naturally inspired structures, the most exciting areas are where technologies and manufacturing paradigms integrate into practical, reliable, and sustainable solutions. These situations are often where engineers and designers from widely different backgrounds can collaborate on projects that range from fundamental material design and characterization to machine development and processing optimization, often transcending previous technological challenges similar to those described herein. Often with such efforts, high-level concepts that seem unachievable can be transferred into commonplace applications that benefit society and our understanding of the world around us. We anticipate that the future will heavily involve multidisciplinary efforts to translate these natural design paradigms into readily manufacturable solutions. Continued efforts towards this goal will result in extensive fruits in academia and industry.

4. Author statement

Profs. Amit Bandyopadhyay conceived the idea and developed the manuscript with graduate student Kellen Traxel. The manuscript contribution came from both authors.

Amit Bandyopadhyay Conceptualization, Supervision, Funding acquisition, Writing - Reviewing and Editing.

Kellen D. Traxel Writing - Original draft preparation, Reviewing and Editing.

5. Acknowledgements

Authors would like to acknowledge financial support from the National Science Foundation under grant number NSF-CMMI 1934230 (PI - Bandyopadhyay), and the National Institute of Arthritis and Musculoskeletal and Skin Diseases of the National Institutes of Health under Award Number R01 AR067306-01 (PI - Bandyopadhyay). The content is solely the authors' responsibility and does not necessarily represent the official views of the National Institutes of Health.

6. References

[1] UGK. Wegst, H. Bai, E. Saiz, A.P. Tomsia, R.O. Ritchie, Nat. Mater. (2015).

[2] Y. Sha, L. Jiani, C. Haoyu, R.O. Ritchie, X. Jun, Int. J. Mech. Sci. 149 (2018) 150–163.

[3] E. Munch, ME Launey, D.H. Alsem, E. Saiz, A.P. Tomsia, R.O. Ritchie, Science (80-.).

(2008).

[4] H. Gao, B. Ji, I.L. Jager, E. Arzt, P. Fratzl, Proc. Natl. Acad. Sci. 100 (2003) 5597–5600.

[5] V. Naglieri, B. Gludovatz, A.P. Tomsia, R.O. Ritchie, Acta Mater. (2015).

[6] V. Naglieri, H.A. Bale, B. Gludovatz, A.P. Tomsia, R.O. Ritchie, Acta Mater. (2013).

[7] G. Zyla, A. Kovalev, M. Grafen, E.L. Gurevich, C. Esen, A. Ostendorf, S. Gorb, Sci. Rep. 7 (2017) 17622.

[8] J. J. Richardson, M. Bjornmalm, F. Caruso, Science (80-.). 348 (2015) aaa2491–aaa2491.

[9] C. Zhang, DA Mcadams, J.C. Grunlan, Adv. Mater. 28 (2016) 6292–6321.

[10] Z. Gan, MD. Turner, M. Gu, Sci. Adv. 2 (2016) e1600084.

[11] M.-S. Pham, C. Liu, I. Todd, J. Lertthanasarn, Nature 565 (2019) 305–311.

[12] F. Stute, J. Mici, L. Chamberlain, H. Lipson, 3D Print. Addit. Manuf. 5 (2018) 285–291.

[13] A. Bandyopadhyay, KD. Traxel, Addit. Manuf. 22 (2018) 758–774.

[14] A. du Plessis, C. Broeckhoven, I. Yadroitsava, I. Yadroitsev, C.H. Hands, R. Kunju, D. Bhate, Addit. Manuf. (2019).

[15] Y. Yang, X. Song, X. Li, Z. Chen, C. Zhou, Q. Zhou, Y. Chen, Adv. Mater. 30 (2018) 1706539.

[16] ASTM ISO/ASTM52900-15 Standard, (2015).

[17] S. Frølich, J.C. Weaver, M.N. Dean, H. Birkedal, Adv. Eng. Mater. 19 (2017) e201600848.

[18] G. X. Gu, M. Takaffoli, A. J. Hsieh, M. J. Buehler, Extrem. Mech. Lett. (2016).

[19] R. Mirzaeifar, L.S. Dimas, Z. Qin, M.J. Buehler, ACS Biomater. Sci. Eng. (2015).

[20] J. J. Martin, B.E. Fiore, R.M. Erb, Nat. Commun. (2015).

[21] D. Kokkinis, M. Schaffner, A.R. Studart, Nat. Commun. (2015).

[22] F. Liu, T. Li, Z. Jia, L. Wang, Extrem. Mech. Lett. 35 (2020) 100621.

[23] M. Rousseau, A. Meibom, M. Gèze, X. Bourrat, M. Angellier, E. Lopez, J. Struct. Biol. 165 (2009) 190–195.

[24] A. Bandyopadhyay, KD. Traxel, C. Koski, S. Bose, in: Addit. Manuf., 2019.

[25] A. A. Zadpoor, J. Malda, Ann. Biomed. Eng. 45 (2017) 1–11.

[26] M. A. Velasco, Y. Lancheros, D. A. Garzón-Alvarado, J. Comput. Des. Eng. 3 (2016) 385–397.

[27] N. N. Zein, I. A. Hanouneh, P. D. Bishop, M. Samaan, B. Eghtesad, C. Quintini, C. Miller, L. Yerian, R. Klatte, Liver Transplant. 19 (2013) 1304–1310.

[28] M. Ziaee, N.B. Crane, Addit. Manuf. 28 (2019) 781–801.

[29] F. Dini, S.A. Ghaffari, J. Jafar, R. Hamidreza, S. Marjan, Met. Powder Rep. 75 (2020) 95–100.

[30] G. X. Gu, F. Libonati, S.D. Wettermark, M.J. Buehler, J. Mech. Behav. Biomed. Mater. 76 (2017) 135–144.

[31] L. S. Dimas, G.H. Bratzel, I. Eylon, M. . Buehler, Adv. Funct. Mater. 23 (2013) 4629–4638.

[32] P. Tran, T.D. Ngo, A. Ghazlan, D. Hui, Compos. Part B Eng. 108 (2017) 210–223.

[33] Y. Yang, X. Li, M. Chu, H. Sun, J. Jin, K. Yu, Q. Wang, Q. Zhou, Y. Chen, Sci. Adv. (2019).

[34] K. D. Traxel, A. Bandyopadhyay, Addit. Manuf. 34 (2020) 101243.

[35] C. W. Hull, US Pat. 4,575,330 (1986) 1–16.

[36] F. P. W. Melchels, J. Feijen, D.W. Grijpma, Biomaterials 31 (2010) 6121–6130.

[37] M. P. Lee, G. J. T. Cooper, T. Hinkley, G. M. Gibson, M. J. Padgett, L. Cronin, Sci. Rep. 5 (2015).

[38] Y. Sano, R. Matsuzaki, M. Ueda, A. Todoroki, Y. Hirano, Addit. Manuf. (2018).

[39] J. L. Walker, M. Santoro, in: Bioresorbable Polym. Biomed. Appl., Elsevier, 2017, pp. 181–203.

[40] R. Sodian, S. Weber, M. Markert, D. Rassoulian, I. Kaczmarek, T. C. Lueth, B. Reichart, S. Daebritz, Ann. Thorac. Surg. 83 (2007) 1854–1857.

[41] A. Žukauskas, M. Malinauskas, E. Brasselet, S. Juodkazis, in: Micro Nano Technol., 2016, pp. 268–292.

[42] J.-W. Choi, H.-C. Kim, R. Wicker, J. Mater. Process. Technol. 211 (2011) 318–328.

[43] D. Bourell, J.P. Kruth, M. Leu, G. Levy, D. Rosen, A.M. Beese, A. Clare, CIRP Ann. - Manuf. Technol. 66 (2017) 659–681.

[44] T. DebRoy, H. L. Wei, J. S. Zuback, T. Mukherjee, J. W. Elmer, J. O. Milewski, A. . Beese, A. Wilson-Heid, A. De, W. Zhang, Prog. Mater. Sci. 92 (2018) 112–224.

[45] S. M. Tofail, E. P. Koumoulos, A. Bandyopadhyay, S. Bose, L. O'Donoghue, C. Charitidis, Mater. Today 21 (2018) 22–37.

[46] X. Wang, S. Xu, S. Zhou, W. Xu, M. Leary, P. Choong, M. Qian, M. Brandt, Y.M. Xie, S.X. Xiaojian Wang Shiwei Zhou, Wei Xu, Martin Leary, Peter Choong, M. Qian, Milan Brandt, Yi Min Xie., X. Wang, S. Xu, S. Zhou, W. Xu, M. Leary, P. Choong, M. Qian, M. Brandt, Y.M. Xie, S.X. Xiaojian Wang Shiwei Zhou, Wei Xu, Martin Leary, Peter Choong, M. Qian, Milan Brandt, Yi Min Xie., X. Wang, S. Xu, S. Zhou, W. Xu, M. Leary, P. Choong, M. Qian, M. Brandt, Y.M. Xie, Biomaterials 83 (2016) 127–141.

[47] S. Bose, D. Ke, H. Sahasrabudhe, A. Bandyopadhyay, Prog. Mater. Sci. 93 (2018) 45–111.

[48] Z. Wang, C. Wang, C. Li, Y. Qin, L. Zhong, B. Chen, Z. Li, H. Liu, F. Chang, J. Wang, J. Alloys Compd. 717 (2017) 271–285.

[49] X. P. P. Tan, Y. J. J. Tan, CSLSL Chow, S.B.B. Tor, WYY. Yeong, Mater. Sci. Eng. C 76 (2017) 1328–1343.

[50] A. Habib, N. Ahsan, B. Khoda, Procedia Manuf. 1 (2015) 378–392.

[51] J.C. Snyder, C.K. Stimpson, K.A. Thole, D. Mongillo, J. Turbomach. 138 (2016) 051006.

[52] H. Sahasrabudhe, A. Bandyopadhyay, Surf. Coatings Technol. 240 (2014) 286–292.

[53] M. Das, V.K. Balla, D. Basu, I. Manna, T.S. Sampath Kumar, A. Bandyopadhyay, Scr. Mater. 66 (2012) 578–581.

[54] C. Hong, D. Gu, D. Dai, A. Gasser, A. Weisheit, I. Kelbassa, M. Zhong, R. Poprawe, Opt. Laser Technol. 54 (2013) 98–109.

[55] T. Gualtieri, A. Bandyopadhyay, Mater. Des. 139 (2018) 419–428.

[56] H. Sahasrabudhe, R. Harrison, C. Carpenter, A. Bandyopadhyay, Addit. Manuf. 5 (2015) 1–8.

[57] B. Heer, A. Bandyopadhyay, Mater. Lett. 216 (2018) 16–19.

[58] D.C. Hofmann, J. Kolodziejska, S. Roberts, R. Otis, R.P. Dillon, J.-O. Suh, Z.-K. Liu, J.-P. Borgonia, J. Mater. Res. 29 (2014) 1899–1910.

[59] M. Leino, J. Pekkarinen, R. Soukka, in: Phys. Procedia, 2016, pp. 752–760.

[60] T. Petrat, B. Graf, A. Gumenyuk, M. Rethmeier, in: Phys. Procedia, 2016, pp. 761–768.

[61] L. J. Kumar, C.G.K. Nair, Mater. Today Proc. 4 (2017) 11068–11077.

[62] B. Onuike, A. Bandyopadhyay, Mater. Lett. (2019).

[63] H. Masuo, Y. Tanaka, S. Morokoshi, H. Yagura, T. Uchida, Y. Yamamoto, Y. Murakami, Procedia Struct. Integr. 7 (2017) 19–26.

[64] B. L. Boyce, B.C. Salzbrenner, J.M. Rodelas, L.P. Swiler, J.D. Madison, B.H. Jared, Y.-L. Shen, Adv. Eng. Mater. 19 (2017) 1700102.

[65] S. A Khairallah, A. T. Anderson, A. Rubenchik, W. E. King, Acta Mater. 108 (2016) 36–45.

[66] W. E. King, H. D. Barth, V. M. Castillo, G. F. Gallegos, J. W. Gibbs, D. E. Hahn, C. Kamath, A. M. Rubenchik, J. Mater. Process. Technol. 214 (2014) 2915–2925.

[67] C. Teng, D. Pal, H. Gong, K. Zeng, K. Briggs, N. Patil, B. Stucker, Addit. Manuf. 14 (2017) 137–147.

[68] C.-A. Gandin, Comptes Rendus Phys. 11 (2010) 216–225.

[69] J. Akram, P. Chalavadi, D. Pal, B. Stucker, Addit. Manuf. 21 (2018) 255–268.

[70] R. Martukanitz, P. Michaleris, T.A. Palmer, T. DebRoy, Z.K. Liu, R. Otis, T.W. Heo, L.Q. Chen, Addit. Manuf. 1 (2014) 52–63.

[71] L. E. Lindgren, A. Lundbäck, M. Fisk, R. Pederson, J. Andersson, Addit. Manuf. 12 (2016) 144–158.

[72] H. Sahasrabudhe, J. Soderlind, A. Bandyopadhyay, J. Mech. Behav. Biomed. Mater. 53 (2016) 239–249.

[73] K. D. Traxel, A. Bandyopadhyay, Addit. Manuf. 24 (2018).

[74] H. Sahasrabudhe, A. Bandyopadhyay, Jom 68 (2016) 822–830.

[75] B. Heer, A. Bandyopadhyay, Addit. Manuf. 23 (2018) 303–311.

[76] H. Sahasrabudhe, S. Bose, A. Bandyopadhyay, Acta Biomater. 66 (2018) 118–128.

[77] Mirzaali, Nava, Gunashekar, Nouri-Goushki, Doubrovski, Zadpoor, Materials (Basel). 12 (2019) 2735.

[78] D. Barba, E. Alabort, R.C. Reed, Acta Biomater. 97 (2019) 637–656.

[79] R. M Kulin, F. Jiang, K.S. Vecchio, J. Mech. Behav. Biomed. Mater. 4 (2011) 57–75.

[80] S. Tarafder, V. K. Balla, N. M. Davies, A. Bandyopadhyay, S. Bose, J. Tissue Eng. Regen. Med. 7 (2013) 631–641.

[81] J. Parthasarathy, B. Starly, S. Raman, J. Manuf. Process. 13 (2011) 160–170.

[82] C. Koski, B. Onuike, A. Bandyopadhyay, S. Bose, Addit. Manuf. 24 (2018) 47–59.

[83] S. Tarafder, S. Bose, ACS Appl. Mater. Interfaces 6 (2014) 9955–9965.

[84] S. Bose, M. Roy, A. Bandyopadhyay, Trends Biotechnol. 30 (2012).

[85] G. Fielding, S. Bose, Acta Biomater. 9 (2013) 9137–9148.

[86] S. Amin Yavari, R. Wauthle, J. van der Stok, A.C. Riemslag, M. Janssen, M. Mulier, J.P. Kruth, J. Schrooten, H. Weinans, A.A. Zadpoor, Mater. Sci. Eng. C 33 (2013) 4849–4858.

[87] D. Zhao, Y. Huang, Y. Ao, C. Han, Q. Wang, Y. Li, J. Liu, Q. Wei, Z. Zhang, J. Mech. Behav. Biomed. Mater. 88 (2018) 478–487.

[88] A. Zadpoor, Int. J. Mol. Sci. 18 (2017) 1607.

[89] S. Bernard, V. Krishna Balla, S. Bose, A. Bandyopadhyay, J. Mech. Behav. Biomed. Mater. 13 (2012) 62–68.

[90] J. Van Der Stok, O.P. Van Der Jagt, S. Amin Yavari, M.F.P. De Haas, J.H. Waarsing, H. Jahr, E.M.M. Van Lieshout, P. Patka, J.A.N. Verhaar, A.A. Zadpoor, H. Weinans, J. Orthop. Res. (2013).

[91] Y. Hu, F. Ning, W. Cong, Y. Li, X. Wang, H. Wang, Ceram. Int. (2017).

[92] L. Yuan, S. Ding, C. Wen, Bioact. Mater. 4 (2019) 56–70.

[93] R. Wauthle, S.M. Ahmadi, S. Amin Yavari, M. Mulier, A.A. Zadpoor, H. Weinans, J. Van Humbeeck, J.-P. Kruth, J. Schrooten, Mater. Sci. Eng. C 54 (2015) 94–100.

[94] V. K. Balla, S. Bodhak, S. Bose, A. Bandyopadhyay, Acta Biomater. 6 (2010) 3349–3359.

[95] F. Libonati, G.X. Gu, Z. Qin, L. Vergani, M.J. Buehler, Adv. Eng. Mater. 18 (2016) 1354–1363.

[96] A. M. Torres, A. A. Trikanad, C. A. Aubin, F. M. Lambers, M. Luna, C. M. Rimnac, P. Zavattieri, C.J. Hernandez, Proc. Natl. Acad. Sci. U. S. A. (2019).

[97] S. Bose, D. Banerjee, A. Shivaram, S. Tarafder, A. Bandyopadhyay, Mater. Des. (2018).

[98] R. Hedayati, S.M. Ahmadi, K. Lietaert, B. Pouran, Y. Li, H. Weinans, C.D. Rans, A.A. Zadpoor, J. Mech. Behav. Biomed. Mater. 79 (2018) 254–263.

[99] A. Zaheri, J.S. Fenner, B.P. Russell, D. Restrepo, M. Daly, D. Wang, C. Hayashi, M.A. Meyers, P.D. Zavattieri, H.D. Espinosa, Adv. Funct. Mater. 28 (2018) 1803073.

[100] N. Suksangpanya, N.A. Yaraghi, D. Kisailus, P. Zavattieri, J. Mech. Behav. Biomed. Mater. 76 (2017) 38–57.

[101] Y. Sun, W. Tian, T. Zhang, P. Chen, M. Li, Mater. Des. 185 (2020) 108239.

[102] Z. Song, Y. Ni, S. Cai, Acta Biomater. 91 (2019) 284–293.

[103] A. C. Neville, B.M. Luke, J. Insect Physiol. 17 (1971) 519–526.

[104] A. Bigi, M. Burghammer, R. Falconi, M.H.. Koch, S. Panzavolta, C. Riekel, J. Struct. Biol. 136 (2001) 137–143.

[105] R. Yang, A. Zaheri, W. Gao, C. Hayashi, H.D. Espinosa, Adv. Funct. Mater. 27 (2017) 1603993.

[106] B. G. Compton, J.A. Lewis, Adv. Mater. (2014).

[107] J. A. Lewis, Adv. Funct. Mater. 16 (2006) 2193–2204.

[108] D. Correa, A. Papadopoulou, C. Guberan, N. Jhaveri, S. Reichert, A. Menges, S. Tibbits, 3D Print. Addit. Manuf. 2 (2015) 106–116.

[109] H. M. A. Kolken, A.A. Zadpoor, RSC Adv. (2017).

[110] C. de Jonge, H. Kolken, A. Zadpoor, Materials (Basel). 12 (2019) 635.

[111] H. Sahasrabudhe, A. Bandyopadhyay, J. Mech. Behav. Biomed. Mater. 85 (2018) 1–11.

[112] A. Bandyopadhyay, S. Dittrick, T. Gualtieri, J. Wu, S. Bose, J. Mech. Behav. Biomed. Mater. 57 (2016) 280–288.

[113] A. Bandyopadhyay, A. Shivaram, M. Isik, J.D. Avila, W.S. Dernell, S. Bose, Addit. Manuf. 28 (2019) 312–324.

[114] K. Stenberg, S. Dittrick, S. Bose, A. Bandyopadhyay, J. Mater. Res. 33 (2018) 2077–2086.

[115] K. D. Traxel, A. Bandyopadhyay, Addit. Manuf. 31 (2020) 101004.

[116] B. Heer, H. Sahasrabudhe, A.K. Khanra, A. Bandyopadhyay, J. Mater. Sci. 52 (2017) 10829–10839.

[117] C. Crook, J. Bauer, A. Guell Izard, C. Santos de Oliveira, J. Martins de Souza e Silva, J.B. Berger, L. Valdevit, Nat. Commun. 11 (2020) 1579.

[118] X. Zhou, Y. Hou, J. Lin, AIP Adv. 5 (2015) 030701.

[119] O. Giraldo-Londoño, L. Mirabella, L. Dalloro, G.H. Paulino, Comput. Methods Appl. Mech. Eng. 363 (2020) 112812.

[120] S. Thapliyal, M. Komarasamy, S. Shukla, L. Zhou, H. Hyer, S. Park, Y. Sohn, R.S. Mishra, Materialia 9 (2020) 100574.

[121] D. Garcia, Z. Wu, J.Y. Kim, H.Z. Yu, Y. Zhu, Addit. Manuf. 27 (2019) 61–71.

[122] B. Liu, C. Jiang, G. Li, X. Huang, Comput. Methods Appl. Mech. Eng. 360 (2020) 112786.

[123] C. Gobert, E.W. Reutzel, J. Petrich, A.R. Nassar, S. Phoha, Addit. Manuf. 21 (2018) 517–528.

[124] L. Scime, J. Beuth, Addit. Manuf. 25 (2019) 151–165.

[125] X. Qi, G. Chen, Y. Li, X. Cheng, C. Li, Engineering 5 (2019) 721–729.

[126] A. Caggiano, J. Zhang, V. Alfieri, F. Caiazzo, R. Gao, R. Teti, CIRP Ann. 68 (2019) 451–454.

[127] L. K. Grunenfelder, N. Suksangpanya, C. Salinas, G. Milliron, N. Yaraghi, S. Herrera, K. Evans-Lutterodt, S.R. Nutt, P. Zavattieri, D. Kisailus, in: Acta Biomater., 2014.

[128] C. Boyle, I.Y. Kim, J. Biomech. (2011).

[129] E. M. Gerhard, W. Wang, C. Li, J. Guo, I.T. Ozbolat, K.M. Rahn, A.D. Armstrong, J. Xia, G. Qian, J. Yang, Acta Biomater. (2017).

[130] R. M. Cardoso, C. Kalinke, R. G. Rocha, P. L. dos Santos, D. P. Rocha, P. R. Oliveira, B. C. Janegitz, J. A. Bonacin, E. M. Richter, R. .A. Munoz, Anal. Chim. Acta (2020).

[131] P. Gay, D. Blanco, F. Pelayo, A. Noriega, P. Fernández, Procedia Eng. 132 (2015) 70–77.